

AD-A247 915



2

Segmentation of Satellite Imagery Using Hierarchical Thresholding and Neural Networks

J. E. Peak
Computer Sciences Corporation
Monterey, CA 93943-5006

Prepared for:
Atmospheric Directorate
Monterey, CA 93943-5006

DTIC
SELECTE
MAR 12 1992
S B D



Approved for public release; distribution is unlimited. Naval
Oceanographic and Atmospheric Research Laboratory, Stennis Space
Center, Mississippi 39529-5004.

92-06220



92 3 09 158

ABSTRACT

A significant task in the automated interpretation of cloud features on satellite imagery is the segmentation of the image into separate cloud features to be identified. A new technique, Hierarchical Threshold Segmentation (HTS) is presented. In HTS, region boundaries are defined over a range of grayshade thresholds. The hierarchy of the spatial relationships between collocated regions from different thresholds is represented in tree form. This tree is pruned, using a neural network, such that the regions of appropriate sizes and shapes are isolated. These various regions from the pruned tree are then collected to form the final segmentation of the entire image.

ACKNOWLEDGMENTS

The author gratefully acknowledges the support of the sponsor, the Office of Naval Technology, Code 22, Mr. James Cauffman, Program Element 62435N, for making this effort possible.

TABLE OF CONTENTS

1. Introduction 1

2. A New Approach to Segmentation 3

 2.1 Segmentation Using Neural Nets 4

 2.2 Segmentation Using Thresholding 4

 2.3 Proposed Segmentation Using Hierarchical Thresholding 7

3. Cloud Feature Image Segmentation Using Hierarchical Threshold Segmentation 14

 3.1 Data Set Description 14

 3.2 Neural Network Derivation 16

 3.3 Neural Network Performance 18

4. Conclusions 23

References 26

Figures 27



Accession For	
NTIS GRA&I	<input checked="" type="checkbox"/>
DTIC TAB	<input type="checkbox"/>
Unannounced	<input type="checkbox"/>
Justification	
By _____	
Distribution/	
Availability Codes	
Dist	Avail and/or Special
A-1	

SEGMENTATION OF SATELLITE IMAGERY USING HIERARCHICAL THRESHOLDING AND NEURAL NETWORKS

1. Introduction

One of the goals of the Naval Oceanographic and Atmospheric Research Laboratory (NOARL) is the automated interpretation of cloud features on satellite images. Such an image interpreter would be used on Navy ships as an aid to the shipboard Oceanographer/Meteorologist. In previous studies (Peak, 1991a & b), the design for the evolving system has been presented and progressively refined as methods for accomplishing the necessary tasks it must perform have been determined. Briefly, the three main tasks are: 1) isolate any cloud features on the image, 2) identify the features in meteorological terms, and 3) perform an overall image interpretation using the individual cloud features to reveal related weather such as turbulence, sea state, etc.

In past work, the third task of top-level interpretation of cloud features and their interrelationships has been addressed in SIAMES -- the Satellite Image Analysis Meteorological Expert System (Peak, 1989). This frame-based expert system guides a human through the process of identifying and analyzing cloud features seen on a satellite image and reveals the associated sensible weather associated with such features.

The ultimate goal of SIAMES is that it would be incorporated into a completely automated system. In other words, the human user, whose role in the present interactive version is to be the pattern recognizer, will be replaced by an automated pattern recognizer. Such an automated cloud pattern recognizer would have to perform the first two above-stated tasks. Initial work in developing such a system was made in Peak (1991a). In that

study it was shown that feed-forward, back-propagation neural networks could be trained to identify large-scale cloud features (Task 2).

One of the conclusions of Peak (1991b) is that the difficult problem lies not so much in the classification of the various large-scale cloud shapes, but rather in the determination of the cloudy areas that define such shapes. This image segmentation problem (Task 1) became the focus of a study using the Hierarchical Stepwise Optimization technique of Beaulieu and Goldberg (1989) on satellite imagery (Peak 1991c). Only limited success was achieved, partly due to the relatively low resolution (7.5 dpi) of the scenes in the study. The technique performed poorly in regions where separate cloud features were located close together, because the average grayshade of the growing regions tended to cause the separate regions to appear to have the same characteristics, and therefore to be combined.

Peak (1991c) concluded that image segmentation, whether via region-growing or edge detection, should be performed in a way that includes constraints on the size and shape of the emergent segments. The notion of derivation using constraints seems to imply that neural networks could somehow be used. The purpose of this study is to address the image segmentation issue particularly with regard to cloud pattern segmentation using neural networks. It will be shown that the new methodology presented here provides a cloud feature segmentation in which both large- and small-scale features emerge. In addition, the boundaries of

these features retain the high degree of detail necessary for the top-level SIAMES analysis.

2. A New Approach to Segmentation

As indicated in Peak (1991b), there are two approaches to image segmentation. One is region-growing, in which pixels of similar grayshade values are grouped together. The HSWO technique, described in Peak (1991c) is a region-growing approach. Another approach is edge detection, in which differentials of grayshade values are used to indicate boundaries between objects in the image. Typically, some gradient of the grayshade is calculated for each pixel of the image. Strong gradients are then used to indicate edges. The difficulty in this methodology is in how to choose the appropriate gradient strength; i.e., in choosing a threshold above which to accept an edge and below which to ignore an apparent edge. Once a threshold is chosen, the resultant edge map often has false edges associated with interior details of objects or other grayshade gradients not associated with actual object boundaries.

Neither of these techniques, as used in a classical sense, appears to solve the problems associated with isolating cloud features. The problems with HSWO have already been discussed above and in Peak (1991c). Meaningful cloud patterns in a single image may consist of both sharp and weak grayshade gradients. For example, edges of a region of cirrus may be quite diffuse while a strong front may have a relatively sharp edge. The choice of an appropriate edge detection threshold to isolate both

such features would be difficult. Cloud features often contain much interior structure which would cause many extraneous edges.

2.1 Segmentation Using Neural Nets

The difficulty with either of the classical segmentation methods is that they are not performed in an "intelligent" way. An Artificial Intelligence (AI) approach would be to define the regions with the inclusion of constraints about the size and shape of the emergent segments. On the surface, such an attempt at an AI-based segmentation might simply be to define a neural network that accepts the pixel grayshades as inputs, and then outputs whether the pixels should be classified as being in a cloud region or not. Such a network would have as many inputs as there are pixels in the image, and also that many outputs. Because of the large number of pixels in an image, it is clear that such a network would be difficult to train. For example, if the region presented later in this study, which contains 33750 pixels, were used the network would have 67500 total inputs and outputs, not to mention the hidden units. Such a network would be impossible to train, besides which there would not be enough cases on which to train such a large network. Therefore such a direct application of neural networks is not possible. However, other neural network approaches are possible.

2.2 Segmentation Using Thresholding

Before pursuing other ways to apply neural networks to the problem, the discussion here will return to the particular segmentation problems regarding cloud features. Such features

typically consist of clouds of different grayshades. For example, the poleward end front might have deeper convection, and hence brighter clouds, than the equatorward end. Other cloud features might contain brighter regions within a dimmer boundary, or have a sharp, bright boundary on one side and not on the other. Neither of the classical segmentation methods would appear well-able to handle such problems.

To introduce the methodology used in this study, we present a similar problem for illustration. Consider the hypothetical mountain range presented in Fig. 1. The range consists of three mountains: Mt. Hovermale, Tag Crag and Peak's Pike (Fig. 1a). In Fig 2a is the corresponding top-down view of these mountains as they would appear on a topographical map with contours of elevation. How can this range be separated into individual mountains? One cannot simply look for local maxima in elevation (Fig 1b) or 10 apparent mountains emerge. The problem is that some mountains consist of more than one local peak. In the case of Mt. Hovermale, the mountain is easily defined by looking for the overall elevation maximum. Tag Crag, however, has two nearly identical peaks but is classified as a separate mountain because of the significant valley between it and Mt. Hovermale. If that valley were not present, the Tag Crag peaks would simply be included as more of the lesser peaks of Mt. Hovermale. Similarly, Peak's Pike has three local peaks separated from Tag Crag by a valley.

Thus, we separate the mountains not so much by their peaks but by the valleys between them. The problem is that there are valleys between the local peaks of a given mountain as well. An

edge detection method using gradients of height would separate only the peaks that have steep valleys (strong height gradients) between them. The problem is that a deep, but gradual, valley separating two mountains would not correspond to an edge.

The contour map (Fig. 2a) reveals how the mountains might actually be separated. One does not look at the contours around local elevation maxima because they sometimes indicate secondary peaks. Rather, we choose the contours that surround regions that correspond to the contour sizes and shapes we expect a mountain to have. Figures 2b-h depict a breakdown of the closed contour regions in Fig. 2a at progressively higher elevations. Notice that the closed-contour regions at lower elevations always encircle those at higher elevations (we assume no overhanging cliffs). In fact, the hierarchy of regions contained by regions at lower elevations can be represented by a tree structure (Fig. 3).

Each of these closed-contour regions represents a candidate definition (i.e., partial image segmentation) of a mountain. If our notion of a mountain is so strict that only the highest elevation qualifies, then region N (Fig. 2h) would be the only mountain present. If the mountain definition is very general, then any raised ground qualifies and region A (Fig. 2b) is our mountain. The actual case lies somewhere between these extremes.

An intelligence-based analysis of these regions might proceed as follows: Region A is too large, and contains too many local peaks, to be one mountain. Region B is rejected for the same reason. Region C qualifies as a mountain because its size and shape fit our notion of a mountain. Region D is dumbbell-

shaped, and therefore is rejected. Region F is the right size and shape; it also has some local peaks (regions H-M) but not so many that it should be rejected. Region G also fits the size and shape, and has only two local peaks, so it also is accepted. Thus, the three mountains in the range are separated here into regions F (Mt. Hovermale), G (Tag Crag) and C (Peak's Pike).

The key idea in the preceding example is that a simple elevation threshold can be used to outline the different mountain regions as long as you use different thresholds for different mountains. By applying intelligence in the choice of a threshold, i.e. reasoning about the sizes and shapes of emergent regions, the proper threshold can be selected. Such a reasoning process is the basis for the intelligent segmentation methodology presented in the next section.

2.3 Proposed Segmentation Using Hierarchical Thresholding

The example in the previous section leads directly to the methodology proposed here. The technique is called Hierarchical Threshold Segmentation (HTS). The above methodology can be used for segmenting grayshade images if brighter grayshade values can be considered to correspond to higher elevations. As a demonstration of this correspondence, a grayshade image of cloud features is now presented. As will be described later, the images analyzed in this study are subregions taken from GOES-West photographs. An example case (not used in this study) depicting the size and location of this subregion is presented in Figure 4. The subregion is located in the Gulf of Alaska from approximately 130° W to 165° W and from 20° N to 47° N. The example chosen is

taken from the Oct. 1, 1983 GOES-W image (Fig. 5a). This 3 inch x 2 inch image was digitized from a photograph into grayshade values between 0 and 255 at 75 dots-per-inch (dpi) resolution.

Whereas in the mountain example we used progressive elevations, here we use grayshade values. If we choose contours of grayshade in brightness intervals of 10, the 0-255 range yields 25 successive grayshade maps (Fig. 6). The last map in Fig. 6 (grayshade=250) is omitted to save space. As before, a tree is used to depict the spatial relationships between regions at different grayshade thresholds (Fig. 7). The region numbering scheme used here is internal to the computer program to group the distinct regions; the values have no physical meaning. Regions that consist of less than 100 pixels are arbitrarily omitted.

To demonstrate the behavior of Hierarchical Threshold Segmentation on satellite cloud imagery it is useful to follow the progression of various regions. For example, region 9 on threshold 10 envelops a band of mostly disjoint, cumulus cells in the lower right quadrant of the image. By threshold 30, the tree indicates a split into the two subregions 6 and 85 (Fig. 7). From threshold 30 until 60, region 85 gets progressively smaller and finally disappears. Similarly, region 6 disappears by threshold 80 (Fig. 6). For the purpose of cloud feature segmentation, a meteorologist would notice the perceptual grouping of the cells into a line, and would therefore choose region 9 in threshold 10 as the best segmentation of this feature. Such a

complex group of clouds would be difficult to segment correctly using a region-growing or edge-detection scheme.

Another cloud feature a meteorologist would key into is the bright, frontal band across the northwest corner (Fig. 5a). In threshold 10 (Fig. 6), this band is included in a very large region (region 2) that dominates the entire northern two-thirds of the area. As the threshold increases from 10 to 130, subfeatures are progressively separated from the edges of this large region until the frontal band is isolated (region 157, threshold 130). If the thresholding is continued, the frontal band continues to shrink, and small, subregions of the band continue to split off.

To demonstrate the overall image segmentation, the optimal threshold choices for the various branches of the tree are indicated by squares around the region number (Fig. 7). The selections here have been made by the author using his admittedly limited satellite interpretation experience. The first criterion in these selections was to isolate distinct, meteorological features. In ambiguous situations, an attempt was made to select regions that seemed to have some perceptual grouping in favor of those that did not. The point in this study is not so much to accept or reject the author's classifications, but rather to demonstrate that the HTS methodology can learn to perform those classifications. As will be shown, the technique can be trained on any set of cases that conform to alternate classifications than those used here.

The optimum, overall image segmentation is presented in Fig. 5b. The feature numbers correspond to those in squares in Fig. 7. The segmentation does quite well in segmenting the frontal band (area 157 from threshold 130), the large area of stratocumulus (area 2), the vorticity max (area 18), the before-mentioned cumulus band (area 9) and the tropical cloudiness extending northward from the ITCZ (area 230). The segmentation of these areas is not only excellent in terms of matching well with the image, but also in terms of the detail of the segmentation boundaries. The eventual feature identification and SIAMES interpretation should be able to capitalize on such detail.

Other sporadic cumulus regions (areas 184, 229, 174 and 157(60)) are delineated. Whether these areas should be interpreted separately or jointly, or even ignored, is an issue for the subsequent module in the overall system. Similarly, the stratocumulus behind the frontal band is segmented into the three regions 238, 285 and 320. It might be preferable for the segmentation to group this entire area as one region. However, the advantages in overall segmentation outweigh such a minor problem because the feature identifier could be designed to consider such small, nearby regions together rather than separately. When one compares the segmentation here with that accomplished by HSWO (Peak, 1991c, Fig. 9a & b) the improvement is considerable.

The above segmentation was accomplished using human, not machine, intelligence in the selection of the thresholds. The excellent results indicate the potential for such a methodology should an additional method for the intelligent selection of

thresholds be developed. As in the mountain example, such a selection method should make the decision based on information about the sizes and shapes of the emergent cloud regions. To accomplish this task, a neural network is used.

Before discussing how a neural network can be applied to this task, we return to the discussion of threshold trees (Fig. 7). The terminology used here is that a "split" is the point at which a region divides into two or more regions at the next higher threshold. A "limb" or "branch" is a successive progression of regions that do not split between thresholds. The selection of the appropriate segmentation threshold for a region effectively accomplishes a "pruning" of the threshold tree.

To structure this decision process in a fashion that can be addressed by a neural network, we choose to process a tree from its base to its limb ends. All splits from threshold 0 (the entire, original image) to threshold 10 are always accepted. Thus, we begin at threshold 10 to decide whether to prune a limb or split. If no pruning is decided upon, the limbs or splits are followed to threshold 20 in the tree and the pruning issue is again decided.

Upon examination of many threshold trees and the segmentation regions they describe, a heuristic for the pruning of certain limbs has emerged: when a limb terminates due to its representative regions shrinking in size to less than 100 pixels, or by such a limb extending to the maximum threshold (250) without splitting, the limb is automatically pruned just after its latest split. For example, the limb in Fig. 7 that begins at region 18

in threshold 20 is automatically pruned at that point. Often, the pruning of a split leaves a limb which is then automatically pruned again back to the point just after the last split.

Once the above heuristic is accepted, all that remains is to decide whether to accept a split or to prune it. This decision is the one which a neural network will make. Since we want the network to make the decision based on the size and shape of the emergent regions, the network inputs are chosen to reveal such information. The first input, indicating the size of a region, is simply the number of pixels contained in the region. The shape of a region is more difficult to define. The actual shape of standard cloud regions such as fronts or vortices may be quite different from case to case. Thus, we avoid using direct measures of shape that might prevent the network from applying to generalized cases. Rather, we have developed two shape indicators that appear to work very well in indicating representative shape characteristics rather than actual shapes. The first of these indicators is the length of the region boundary, the number of pixels on the perimeter. The second shape indicator is the ratio of the number of pixels in the region to the number of boundary pixels. This ratio is referred to here as the "fractal dimension" because, like a fractal dimension, it expresses the complexity of a region (fractal) boundary relative to its size. Here a smaller fractal dimension indicates a more complex region boundary.

The neural network needs information about the regions both before and after a potential split. If all splits were from one

region into two regions, we could simply include the three above-stated parameters for the region prior to the split and for the two regions after the split; a total of nine parameters. However, sometimes a split leads to multiple subregions. Because the neural network can only accept a fixed number of inputs, in those situations we provide the network with the parameters for the two largest of these potential subregions. The complete network configuration will be described later.

In the next section, a data set of cases for training the network will be presented. The neural network architecture will be chosen, and the HTS technique will be tested on both dependent and independent data.

Before proceeding, the steps in the Hierarchical Threshold Segmentation procedure are summarized:

1. Start with a grayshade (0-255) image.
2. Partition the image into regions of contiguous pixels with grayshade values above a given threshold.
3. Do this partitioning for thresholds every 10 grayshade values (10, 20, 30, ..., 240, 250).
4. Construct a tree in which regions at higher thresholds limb or split from regions occupying the same area at lower thresholds.
5. Prune the limbs of the tree:
 - 5.1 Prune from the tree base to the limb ends.
 - 5.2 Start with the regions in the grayshade 10 threshold.
 - 5.3 When a limb terminates with no split, prune it back at the point just after the latest split.
 - 5.4 When a limb splits into two or more limbs use the neural network to decide whether to keep or prune the split.

6. The regions at the ends of the pruned tree limbs are those that best segment the image.

7. Collect these individual region segmentations to form an overall image segmentation.

3. Cloud Feature Image Segmentation Using Hierarchical Threshold Segmentation

3.1 Data Set Description

The cases used in this study are a subset of the GOES_W images used in Peak (1991b). In this study, only the Oct. and Nov. 1983 cases are used. Cases are taken every three days, yielding 21 images. The Oct. 19 image has a particularly bright latitude/longitude grid overlaid on the image which interfered with the HTS technique; therefore this case has been eliminated, reducing the data set to 20 cases. These cases were alternately assigned to dependent and independent samples as summarized in Table 1.

In Peak (1991b), these GOES-W photographic images of the Pacific Ocean were digitized to grayshades at 75 dpi resolution and then averaged to lower resolution for the HSWO tests. Here, the goal is to retain the higher resolution so that the thresholding technique can delineate detailed region boundaries. To keep the amount of data in each case at a smaller, more manageable level, the entire image area was not used here. Rather, a midlatitude subregion, located in the Gulf of Alaska, was used (e.g., Fig. 4). This region covers a 3 inch x 2 inch area on the original image and was chosen because it includes many significant midlatitude cloud features, and because it avoids inclusion

Table 1. Dependent and independent sample cases.

<u>Dependent Sample</u>	<u>Number of Splits</u>	<u>Image & Segmentation</u>	<u>Threshold Tree</u>
Oct. 4	17	Fig. 8	Fig. 9
Oct. 10	8	Fig. 10	Fig. 11
Oct. 16	11	Fig. 12	Fig. 13
Oct. 25	11	Fig. 14	Fig. 15
Oct. 31	9	Fig. 16	Fig. 17
Nov. 6	6	Fig. 18	Fig. 19
Nov. 12	11	Fig. 20	Fig. 21
Nov. 18	11	Fig. 22	Fig. 23
Nov. 24	8	Fig. 24	Fig. 25
Nov. 30	9	Fig. 26	Fig. 27

Total Dependent Splits 101

<u>Independent Sample</u>	<u>Number of Splits</u>	<u>Image & Segmentation</u>	<u>Threshold Tree</u>
Oct. 1	13	Fig. 5	Fig. 7
Oct. 7	13	Fig. 28	Fig. 29
Oct. 13	15	Fig. 30	Fig. 31
Oct. 22	5	Fig. 32	Fig. 33
Oct. 28	8	Fig. 34	Fig. 35
Nov. 3	8	Fig. 36	Fig. 37
Nov. 9	8	Fig. 38	Fig. 39
Nov. 15	12	Fig. 40	Fig. 41
Nov. 21	13	Fig. 42	Fig. 43
Nov. 27	10	Fig. 44	Fig. 45

Total Independent Splits 105

Total Splits 206

of any coastlines which are artificially outlined on these photographs. At 75 dpi the region has 225 x 150 pixels, or a total of 33750 grayshade values in each image.

For the images listed in Table 1, the Gulf of Alaska subregions were isolated. These 20 cases are depicted in the Figures listed in Table 1. As in Fig. 6, HTS was applied at increments of 10 grayshade values. Figures of the hierarchical threshold regions, such as those for the Oct. 1 case depicted in Fig. 6,

will not be shown here for the remaining 19 cases (to save space). The resultant threshold trees for the 20 cases are depicted in the Figures listed in Table 1. The optimal pruning points, as outlined by squares in the trees, lead to an ideal segmentation for each case. These segmentations are depicted directly beneath each image in the Figures listed in Table 1. Each split in the 20 threshold trees becomes a case in the data sets for training and testing the neural network. This process will be described in the next section.

3.2 Neural Network Derivation

In Section 2.3, nine potential inputs from each case for the neural network were presented. As in Peak (1991b), discriminant analysis will be used to reduce the number of inputs to the neural network. In previous experiments such a reduction has led to improved network performance while requiring fewer training cases.

The results of the stepwise discriminant analysis, using all 206 cases, are presented in Table 2. The terminology used here is that the region before the split is the "parent" while the two regions it is split into are the "child" regions. The larger of

Table 2. Order of entry of variables into stepwise discriminant analysis of cases in Table 2. The symbol # refers to number or count.

<u>Entry Number</u>	<u>Variable</u>	<u>F-to-Enter</u>
1	# child 1 pixels	245.81
2	parent fractal dim.	52.92
3	# parent boundary	8.67
4	child 1 fractal dim.	1.12
5	# child 2 boundary	8.00

the two is always designated "child 1" and the smaller, "child 2." The most significant parameter (e.g., having the largest F-to-Enter ratio) affecting the decision to split is the number of pixels in child 1 (Table 2). The second-most significant predictor is the fractal dimension of the parent region. Additional important information is the number of parent boundary pixels and the child 1 fractal dimension (Table 2). The number of boundary pixels is the only predictor included that pertains to child 2.

The discriminant analysis reduces the number of inputs from nine to only five. Using the heuristic that we need as many training cases as the number of inputs plus the number of outputs times five, we need a minimum of five plus two times five, or 35 cases. Here we have 101 cases in the dependent sample (Table 1) which is clearly sufficient for training the neural network.

As in Peak (1991a & b), we use a feed-forward, backpropagation neural network. The network configuration chosen is depicted in Fig. 46. The network has the five above-mentioned inputs. The first hidden layer has 10 units while the second hidden layer has four units (Fig. 46). This configuration was arbitrarily chosen and may not represent the optimal choice. The network has two outputs: one corresponding to the decision to prune and another corresponding to the decision not to prune.

The neural network was derived using the DESIRE/NEUNET software (Korn, 1989) on an IBM-PC 386/25 clone. The network converged very quickly, after about 200 iterations, requiring

less than one minute of computer time. In the next section, this network will be tested on the dependent and independent samples.

3.3 Neural Network Performance

The neural network was used to prune the threshold trees of the dependent and independent cases (odd numbered Figures 7-45). As mentioned earlier, the optimal pruning points are indicated in these figures by a box around the terminal node in each limb. If the neural network selection disagrees with the optimal selection, a circle is drawn around the neural network pruning point. Thus, if the network performs perfectly, the threshold tree is simply the optimal tree with only boxes and no circles.

The final step in Hierarchical Threshold Segmentation is to group the regions from all of the pruned branch ends into an overall segmentation. These segmentations for the optimally-pruned trees are depicted immediately below the satellite image for each case (Figures 5b & even-numbered Figures 8b-44b). Each region is numbered to correspond to the regions on the threshold tree. When the neural network disagrees with the optimal pruning, an additional Figure "c" is added to these figures to show the different tree segmentation. Only the regions that differ from the optimal segmentation are numbered in these figures. For example, the Oct. 1 case (Fig. 5a) results in the threshold tree depicted in Fig. 7. The neural network differs from the optimal selection in that it chooses to prune the split of region 145 at threshold 120, while the optimal pruning is to keep the split into regions 157 and 320 at threshold 130 (Fig. 7). In the optimal segmentation (Fig. 5b), regions 157 and 320 are depicted.

In the tree segmentation (Fig. 5c), region 145 is depicted and numbered to indicate where the tree differs from the optimal segmentation. The remaining, unnumbered regions in Fig. 5c are identical to those in Fig. 5b. In this way, any time a third figure appears, the exact error made by the tree can easily be seen.

Of the 10 dependent sample cases, the tree prunes perfectly six cases: Oct. 4 (Figs. 8 & 9), Oct. 16 (Figs. 12 & 13), Oct. 25 (Figs. 14 & 15), Oct. 31 (Figs. 16 & 17), Nov. 6 (Figs. 18 & 19) and Nov. 30 (Figs. 26 & 27). These six cases contain a total of 63 splits. Four cases contain errors: Oct. 10 (Figs. 10 & 11), Nov. 12 (Figs. 20 & 21), Nov. 18 (Figs. 22 & 23), Nov. 24 (Figs. 24 & 25). While these four cases contain a total of 32 splits, there are only a few erroneous splits. The Oct. 10 and Nov. 12 cases have two errors each, while the Nov. 18 and Nov. 24 cases each have one error. Thus, out of 101 dependent sample cases there is a total of six incorrect pruning selections by the neural network, an accuracy rate of 94%.

In the Oct. 10 case the neural network prunes the tree (Fig. 11) at node 93 (threshold 70) which deletes two later splits that should be kept. In the actual case, it can be seen that the optimal pruning segmented the cellular clouds of regions 85 and 177 as being separate from the more solid clouds of region 97(130). However, there appears to be a perceptual grouping of these regions in that they all have a common curvature (Fig. 10a). Thus, the tree segmentation of region 93 (Fig. 10c) could be interpreted as correct.

The Nov. 12 case includes two separate errors: the failure to retain the split of region 33, threshold 70 into regions 41 and 168 (Fig. 21) and the inclusion of the split of region 83, threshold 90 into regions 81 and 210. The former region split was based on the different cumulus cell size to the west of the central cloud mass (region 41) (Figs. 20a & b). It might be argued that this split is unnecessary. The latter split separates the eastern portion of a warm front (region 81, Fig. 20c) from the comma cloud system to the west (region 210). Again, the different texture of these regions might support their separation such that the effect of the neural network error is minimized.

A similar error occurs in the Nov. 18 case. Here, region 63, threshold 130 (Fig. 23) is erroneously split into subregions 113 and 169 (see Figs. 22b & c). In the author's opinion, these small, ragged cloud regions should remain included in the large cloud band 113. However, the error should not effect the classification of the cloud band and the two, small cloud regions could easily be ignored as being insignificant by the later feature identifier.

The final, dependent sample error occurs in the Nov. 24 case. Region 173, threshold 50 (Fig. 25) is erroneously divided into regions 168 and 196. As can be seen in Fig. 24, the small region 168 should probably remain included in the prefrontal cloudiness of region 173. Again, the error does not appear to be serious.

Of the 10 independent sample cases, the tree prunes perfectly five cases: Oct. 22 (Figs. 32 & 33), Nov. 3 (Figs. 36 & 37),

Nov. 15 (Figs. 40 & 41), Nov. 21 (Figs. 42 & 43) and Nov. 27 (Figs. 44 & 45). These five cases contain a total of 48 correct splits. Five cases contain errors: Oct. 1 (Figs. 5 & 7), Oct. 7 (Figs. 28 & 29), Oct. 13 (Figs. 30 & 31), Oct. 28 (Figs. 34 & 35) and Nov. 9 (Figs. 38-39). Considering that these five cases contain a total of 57 splits, the number of erroneous splits is quite small. The Oct. 7 case has three errors and the Oct. 1, 13, 28 and Nov. 9 cases each have only one error. Thus, out of 105 independent sample cases there is a total of only seven incorrect pruning selections. The neural network accuracy rate for these independent cases is 93%; nearly as good as for the dependent sample.

As indicated earlier, the error of the Oct. 1 case is that the neural network chooses to prune the split of region 145, threshold 120 rather than to keep the split into regions 157 and 320 (Fig. 7). As seen in most of the previous errors, the error results from inclusion of an adjacent area of cellular clouds (region 320) into a region of solid clouds (region 157).

The three errors in the Oct. 7 case result from the neural network pruning two branches too early. That region 92 (Fig. 28c) is selected rather than the two regions 103 and 110 (Fig. 28b) is probably not serious, although the image (Fig. 28a) seems to indicate two, separate cloud bands in the stratocumulus. Similarly, the failure to split region 27 (Fig. 28c) into the three subregions 21, 40 and 43 (Fig. 28b) is a judgment call due to the complexity of this cloud pattern (Fig. 28a).

The error in the Oct. 13 case is to prune the branch with region 7, threshold 10 (Fig. 31) too early. This is the only error on this case, which means that the network would have correctly allowed the four subsequent splits in the tree. These splits never occur because the tree is pruned from the base to the limbs. In most cases, pruning in this direction results in better segmentations; this case happens to be an exception. One reason that area 7 (Fig. 30c) is not split may be due to its location along the lower edge of the grid, which creates an artificial boundary. If the remaining cloud area south of the boundary were included, the network inputs might better represent its shape.

In the Oct. 28 case, region 8 (Fig. 34b) is split into subregions 9 and 137 (Fig. 34c). The author's opinion was that this feature should be segmented as a continuous cloud band. However, the change in orientation of region 137, and its different texture might indicate that it should indeed be a separate feature.

Finally, the Nov. 9 case has a very complex set of cloud lines trailing from a cold front (Fig. 38a). The neural network fails to include the brightest of these bands (region 188, Fig. 38c) as part of the front (region 2, threshold 50). The majority of the front is still included in the latter area, so this error is not serious.

It should be emphasized that, although the high accuracy of the neural network is gratifying, it pertains only to the neural network's ability to prune the threshold trees into the "optimal"

classifications it was trained on. The accuracy of Hierarchical Threshold Segmentation in terms of the methodology being able to segment cloud features can only be judged subjectively by an expert in the identification of cloud features on an image. The author's opinion is that the segmentations are quite good; however, readers are invited to peruse these cases and judge for themselves the capability of HTS. Because the neural network can be trained on any set of cases, alternate expert opinion could be used to provide different optimal classifications, if desired, for training.

4. Conclusions

A new methodology, called Hierarchical Threshold Segmentation (HTS), is presented as a means to partition images of cloud patterns into features for later identification and interpretation. The technique involves applying a threshold to the image at progressive thresholds of grayshade value. The sequence of emergent regions is depicted in a tree structure which is pruned heuristically and with a neural network. The regions at the ends of the tree branches are combined to form an overall image segmentation.

The neural network that accomplishes the tree pruning is trained on 101 cases of tree branch splits. Inputs to the network include information about the region sizes (pixel counts), region boundaries (boundary pixel counts), and shape complexity in the form of a "fractal dimension" (ratio of size to boundary length). The network accuracy for the dependent sample is 94%, with independent sample (105 cases) accuracy of 93%. As dis-

cussed in the text, the few erroneous cases do not seriously affect the segmentation.

The true performance of HTS is in determining whether the resultant segmentations delineate cloud features of interest. The author's subjective opinion is that it does for these cases. Both large- and small-scale features emerge. The segmented areas retain a large degree of boundary and internal detail; such information will likely be crucial in the ability to identify these regions and interpret their meteorological significance. The ultimate test of HTS's segmentation skill will come when the technique becomes part of a completely automated image interpretation system. Most readers will agree that these segmentations are far superior to those depicted in Peak (1991c) using Hierarchical Stepwise Optimization.

In future studies, the technique should be tested on other areas such as the tropics. The system was tested here on only open ocean cases. HTS might have difficulty if ice shelves or land are present; however, such problems occur with region-growing or edge-detection segmentation as well.

A larger analysis area will also be necessary for the eventual HTS module of the automated image interpretation system. Because HTS is not as sensitive to grayshade gradients as is edge detection, it might even be possible to apply it to mosaiced imagery from multiple polar-orbiter passes. Even if the emergent regions delineate the edge between passes, the neural network could be trained to ignore such straight-line separations. Thus, HTS might solve the limited-swath problem that has caused this

research effort to focus on GOES data until now rather than the polar-orbiters that will be available through TESS(3).

The technique has the most difficulty in handling adjacent regions of clouds with different textures. The neural network pruning technique should therefore include textural information about the regions to improve such decisions.

As HTS is tuned and improved, methods for ignoring small cloud features or grouping distinct features that have a perceptual grouping might be explored. For example, another level of hierarchy might be applied in which only the most significant region is isolated, its pixels removed from consideration, and the process repeated with the remaining pixels.

It is recommended that further HTS experiments be performed to address some of these remaining issues. A prototype automated image analysis system could then be built by linking an HTS module with a feature identification module, and eventually a SIAMES module, to perform an automated image analysis.

REFERENCES

- Beaulieu, J.-M. and M. Goldberg, 1989: Hierarchy in picture segmentation: A stepwise optimization approach. IEEE Trans. on Patt. Anal. and Mach. Intell., Vol. 11, No. 2, 150-163.
- Korn, G. A., 1989: Interactive Dynamic System Simulation. McGraw-Hill, New York, NY, 194 pp.
- Peak, J. E., 1989: Initial Expert Evaluation and Resultant Modifications to the Satellite Image Analysis Meteorological Expert System (SIAMES) Prototype. Naval Oceanographic and Atmospheric Research Laboratory, Atmospheric Directorate, unpublished internal report, Monterey, CA, 93943-5006, 12 pp plus appendices.
- Peak, J. E., 1991a: Neural Network Methodologies and Their Potential Application to Cloud Pattern Recognition. Naval Oceanographic and Atmospheric Research Laboratory, Atmospheric Directorate, Technical Note 103, Monterey, CA, 93943-5006, 46 pp.
- Peak, J. E., 1991b: Application of Neural Networks to Large-scale Cloud Pattern Recognition. Naval Oceanographic and Atmospheric Research Laboratory, Atmospheric Directorate, Technical Note 104, Monterey, CA, 93943-5006, 38 pp.
- Peak, J. E., 1991c: Use of Heirarchical Stepwise Optimization for the Segmentation of Cloud Features. Naval Oceanographic and Atmospheric Research Laboratory, Atmospheric Directorate, Technical Note 106, Monterey, CA, 93943-5006, 64 pp.

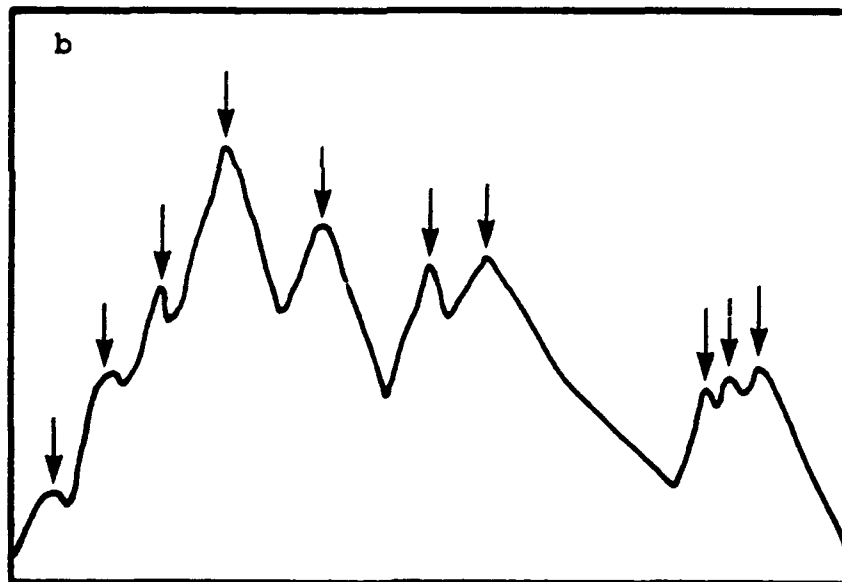
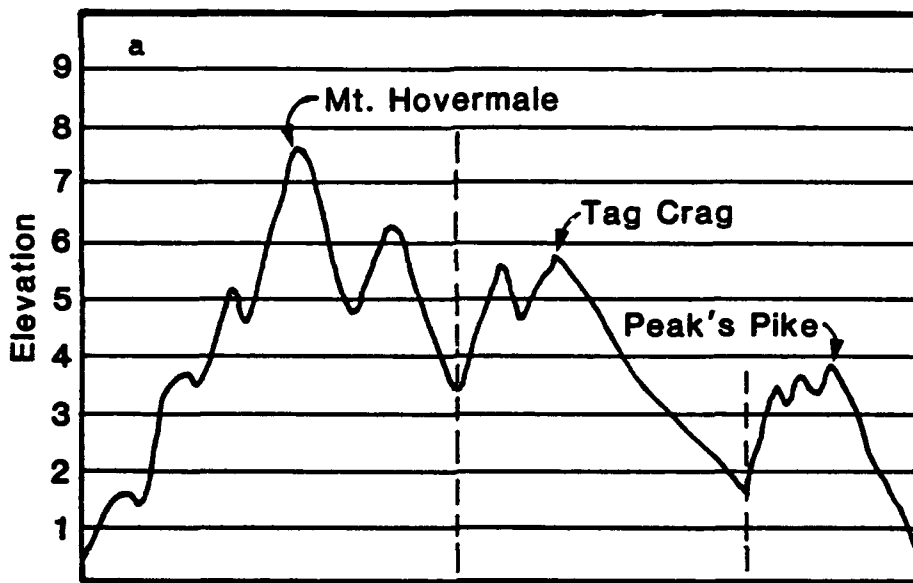


Figure 1. a) Cross-section view of hypothetical mountain range consisting of three separate mountains, and b) the same hypothetical range with local maxima indicated by arrows.

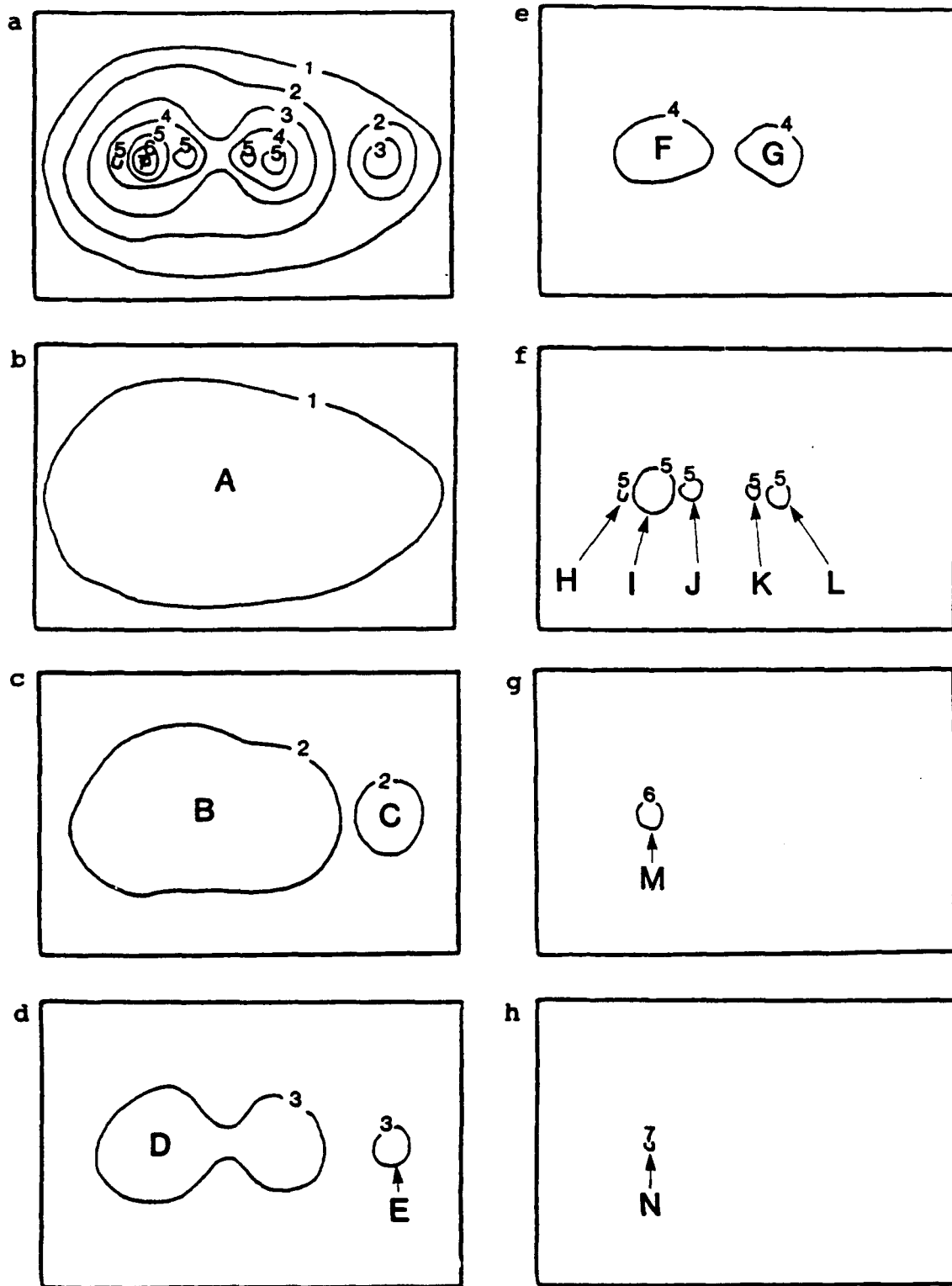


Figure 2. Hypothetical contour map of the mountain range depicted in Fig. 1. Letters A-N indicates regions isolated by being outlined by the various contours.

Elevation

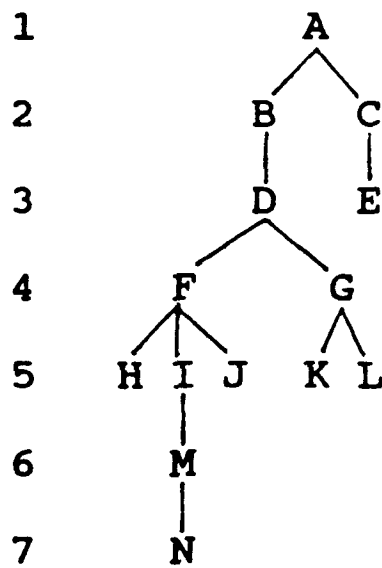


Figure 3. Tree structure representing the hierarchy of closed-contour regions from Fig. 2 (letters A-N). Regions at higher elevations are contained in the regions at lower elevations connected by tree limbs.

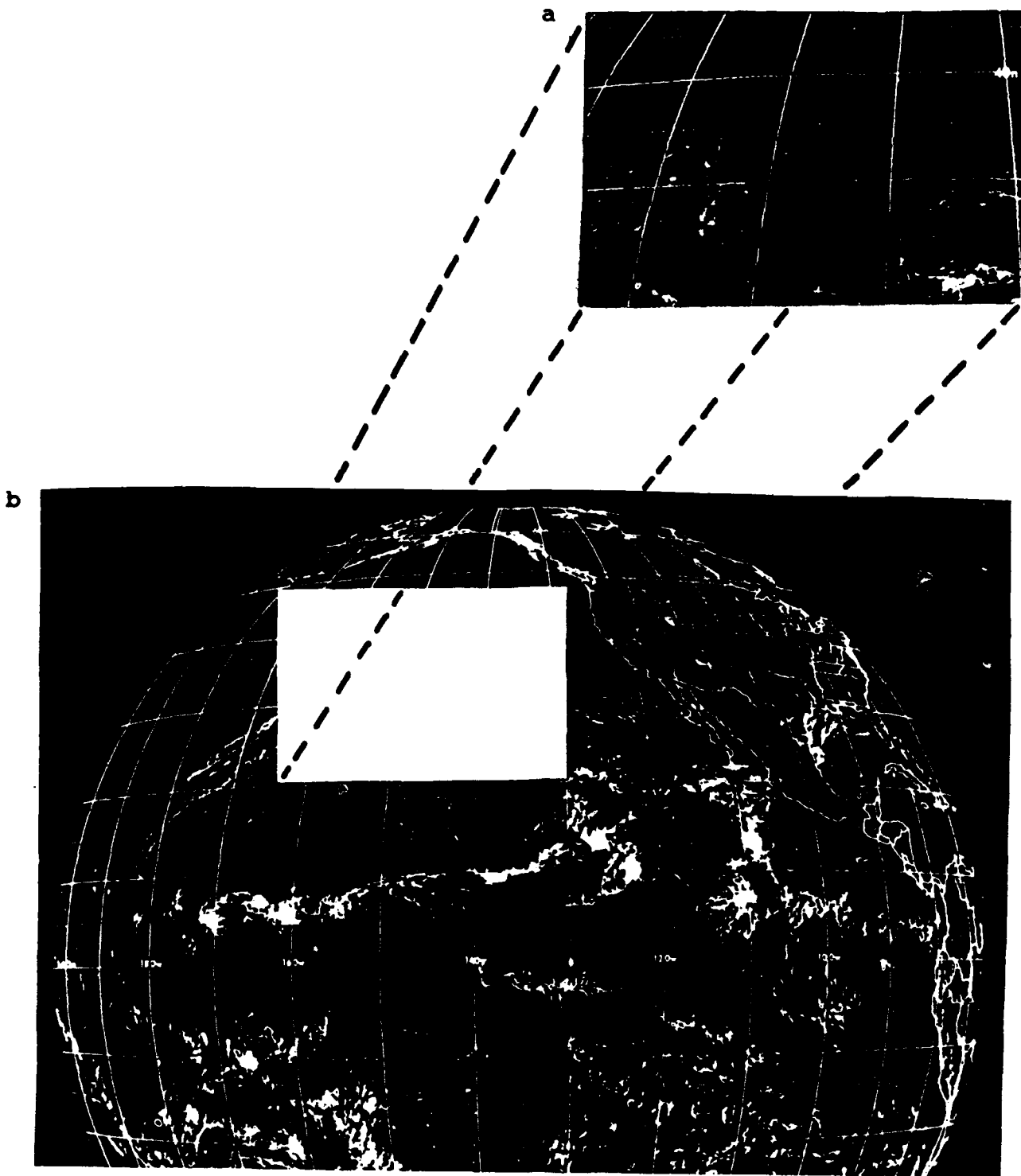


Figure 4. Example GOES-W visual image (b) showing the location from which the subregion used in this study (a) is taken. This case, from January 1982, is presented only as an example and was not used in the study.

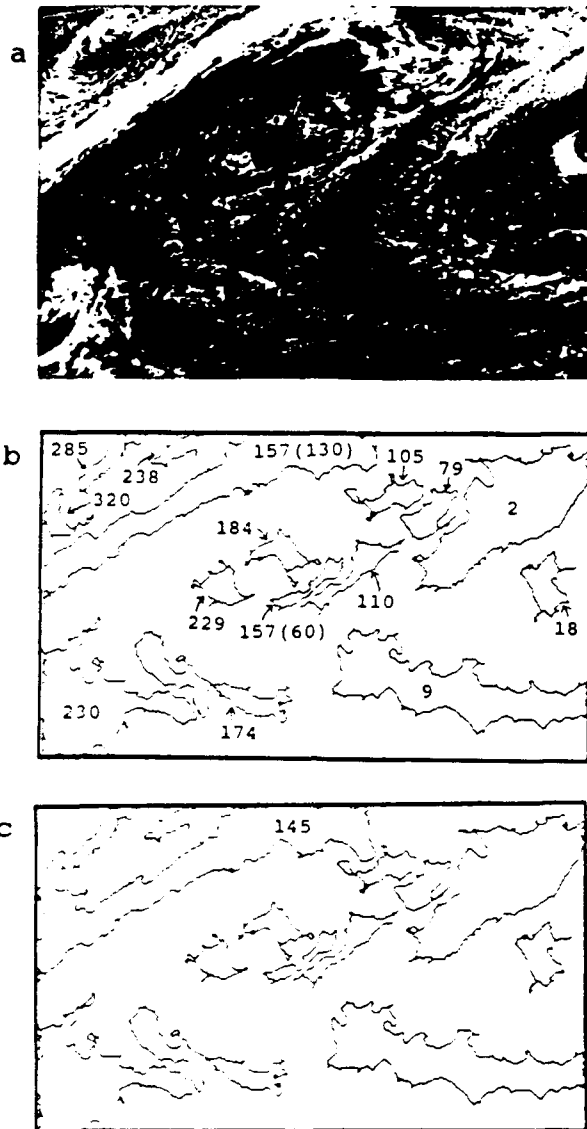


Figure 5. a) Subregion of GOES-W visual image for Oct. 1, 1983 used for digitization and cloud feature segmentation; b) Optimal segmentation of the image in (a) with threshold segmentation regions as numbered; c) hierarchical threshold segmentation of the image in (a) using a neural network to choose the pruning points in the threshold tree (depicted in Fig. 7). Only regions that differ from the optimal choice (shown in b) are numbered in (c).

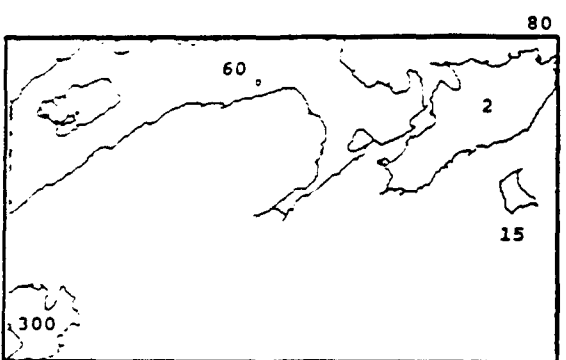
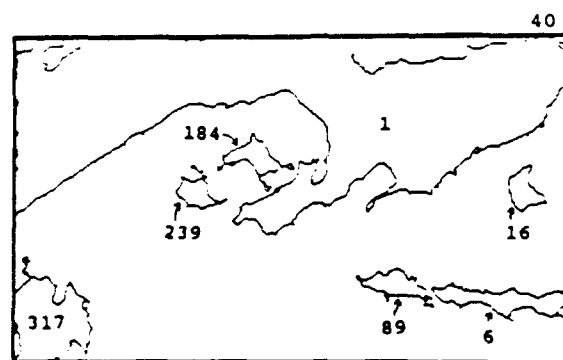
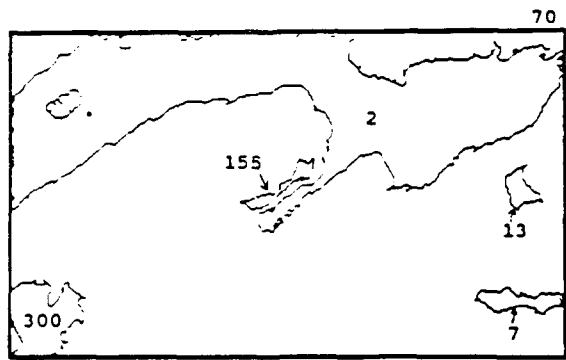
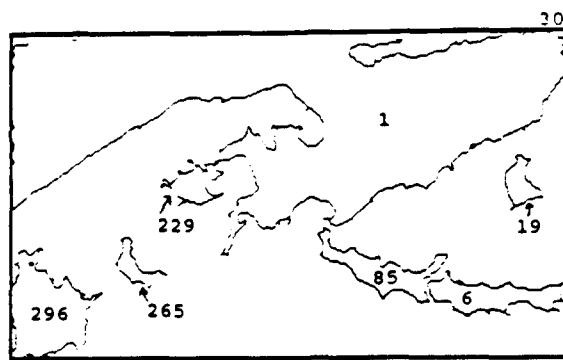
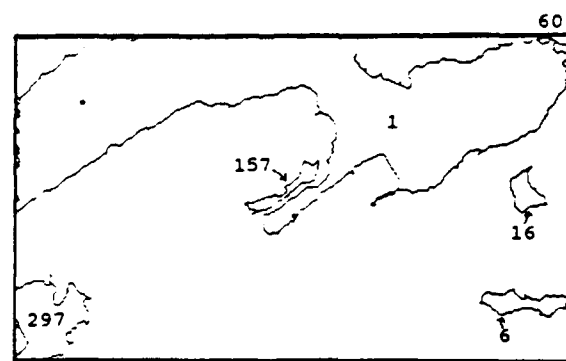
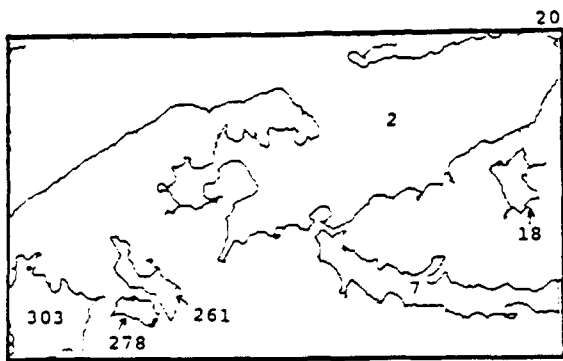
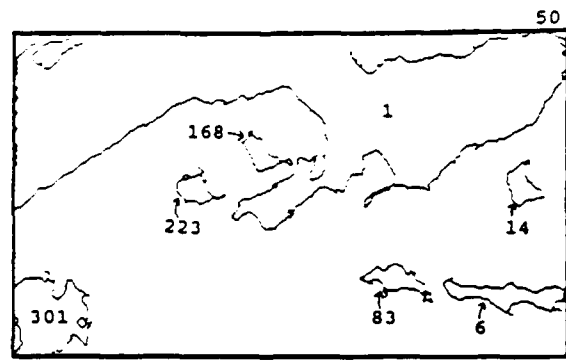
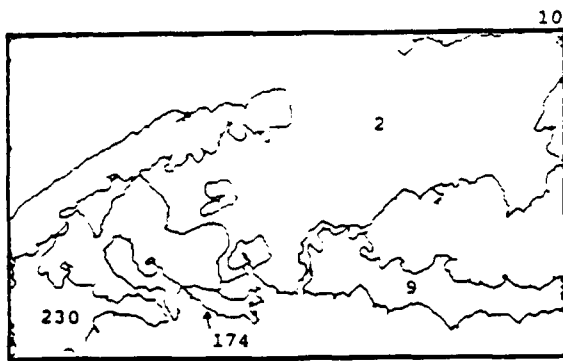


Figure 6. Image segmentation regions at grayshade thresholds 10-240 for the case depicted in Fig. 5. Regions are labeled by numbers generated internally by the hierarchical thresholding program; numerical value is unimportant and may or may not change between successive thresholds.

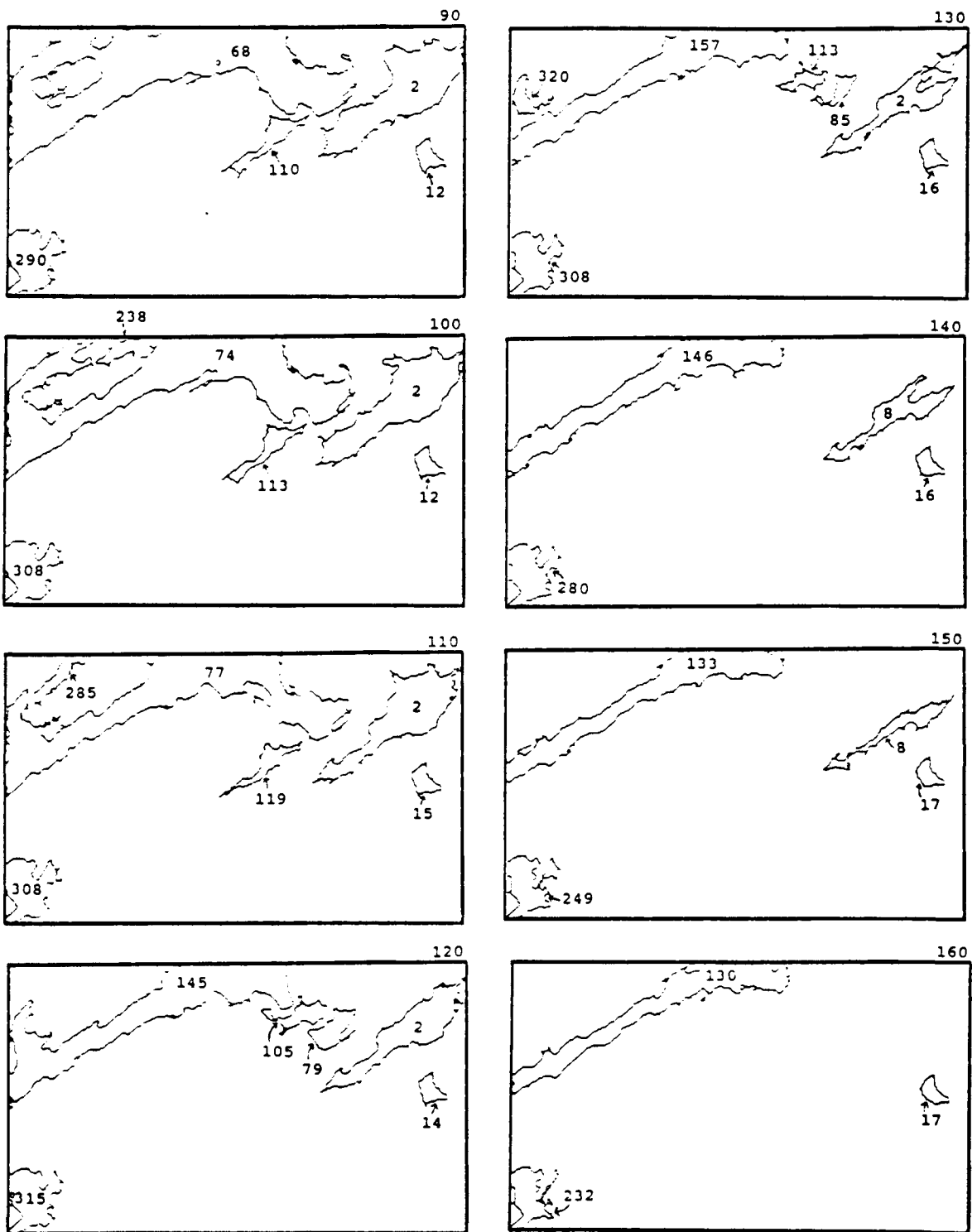


Figure 6 (continued).

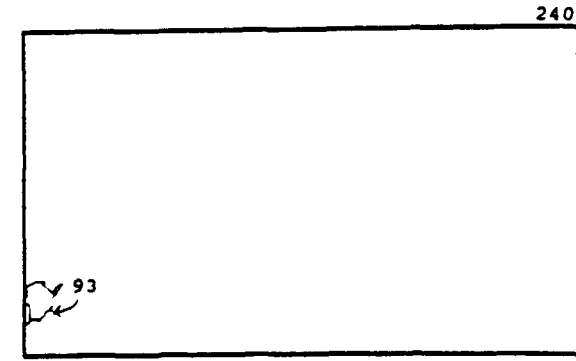
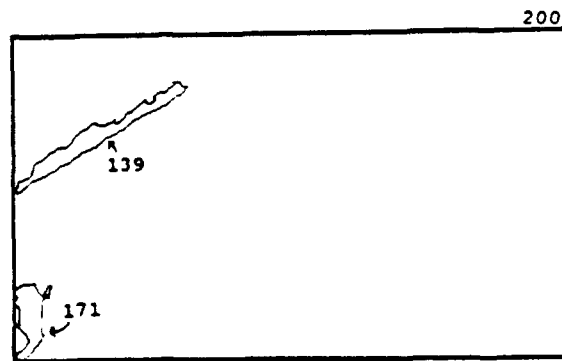
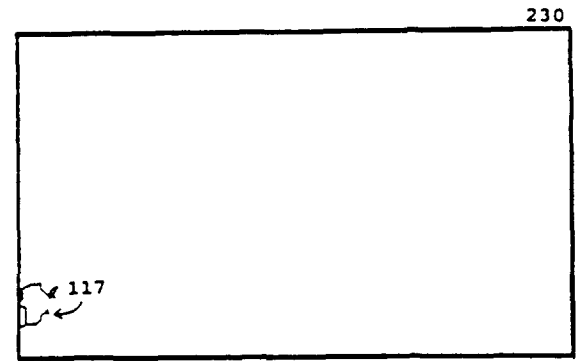
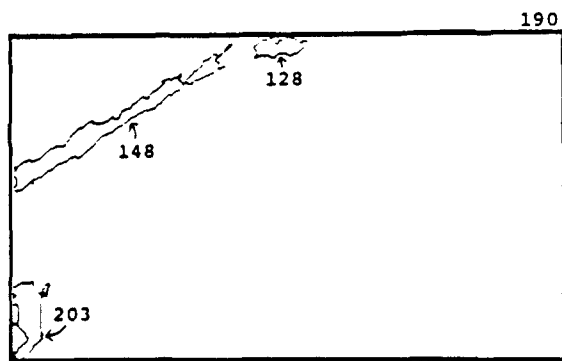
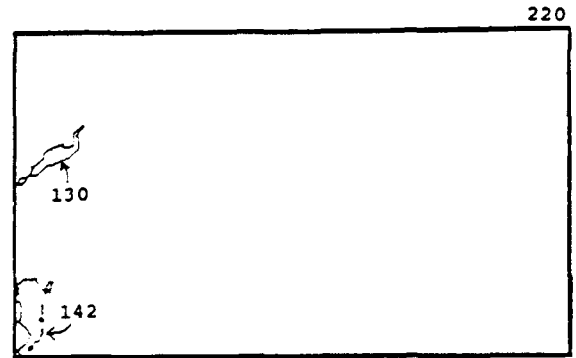
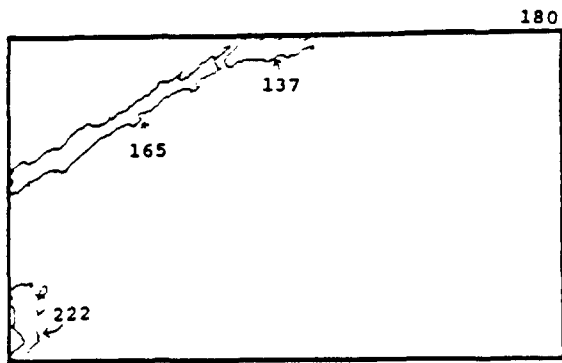
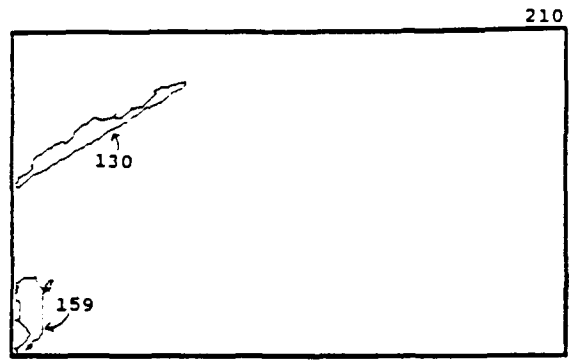
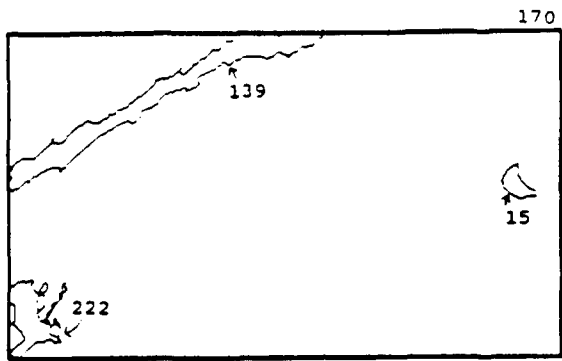


Figure 6 (continued).

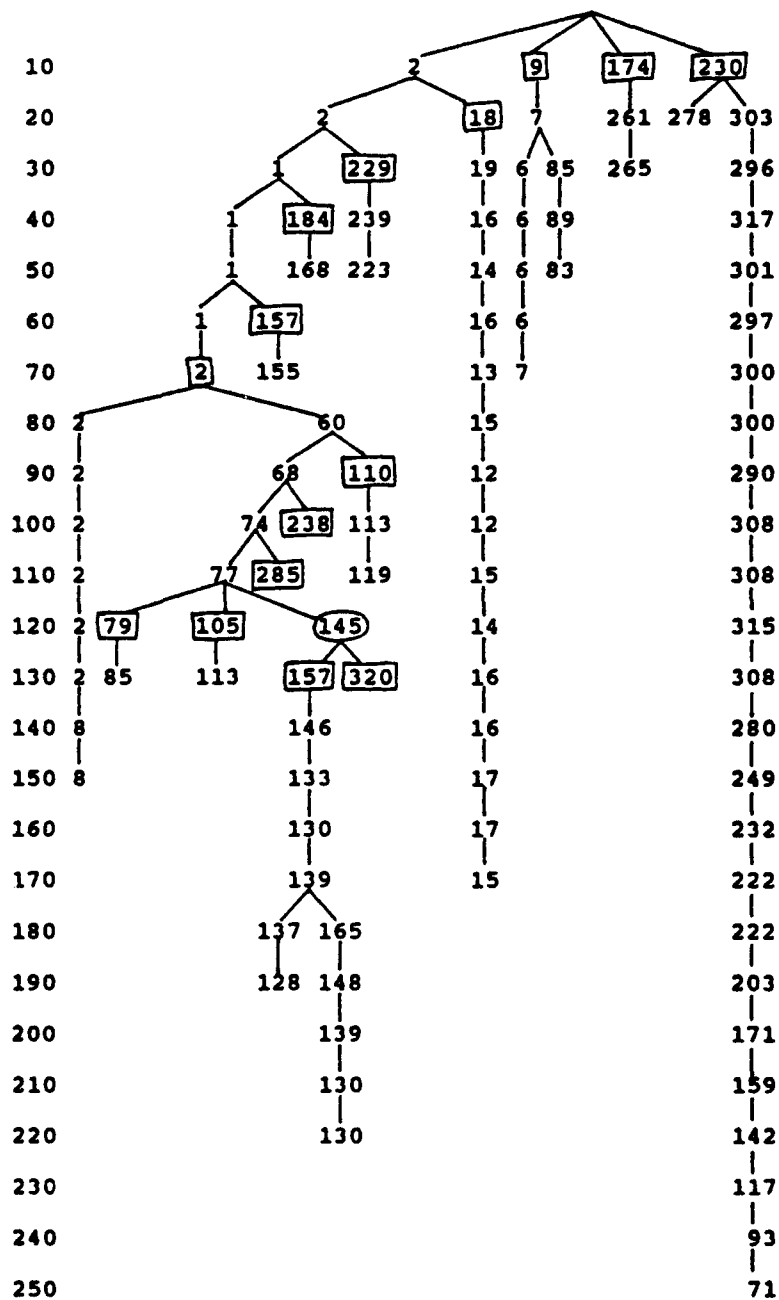
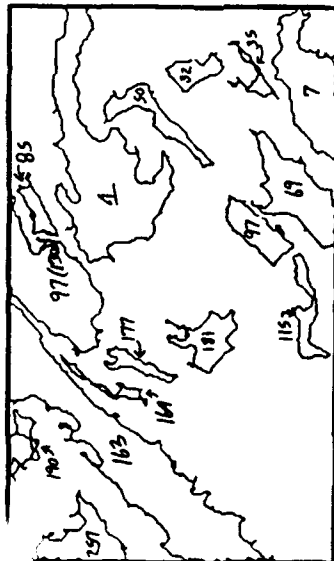


Figure 7. Tree depicting the spatial relationships between regions at successive grayshade thresholds 10-250 (numbers at left.) Region numbers outlined by boxes indicate optimal tree pruning points (depicted in Fig. 5b), whereas those outlined by ovals indicate the neural-network-selected pruning points.

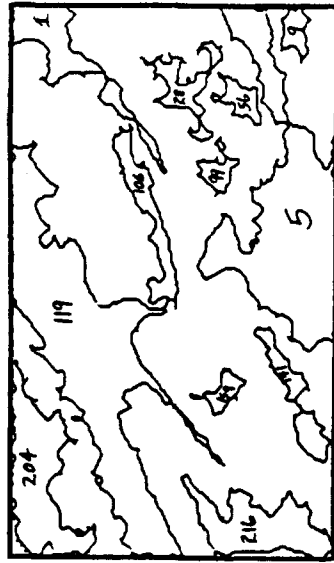


a





a



b

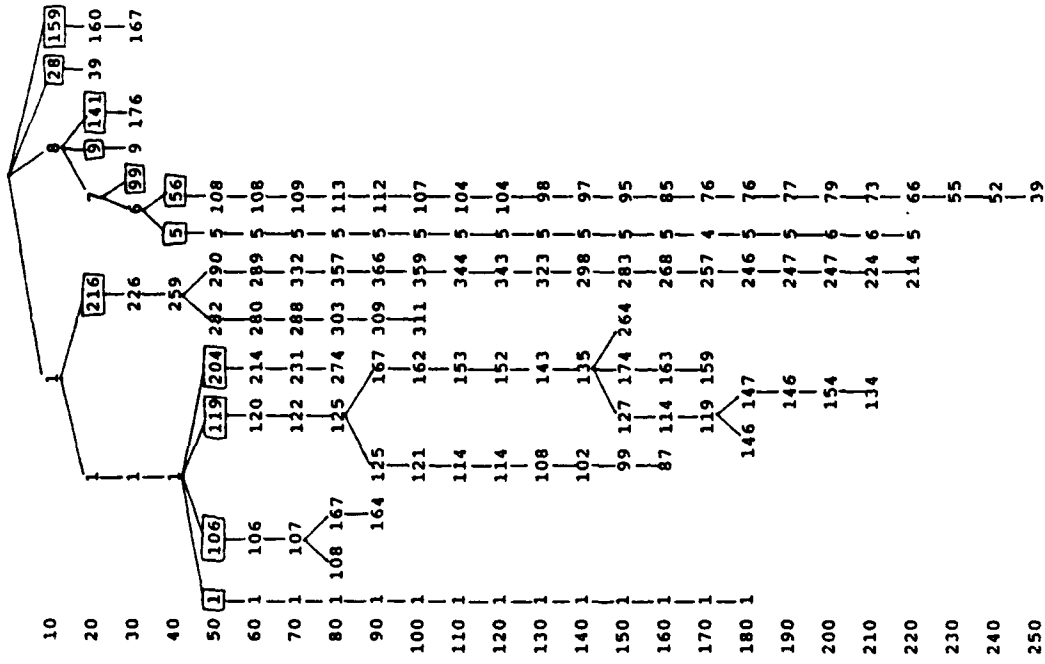
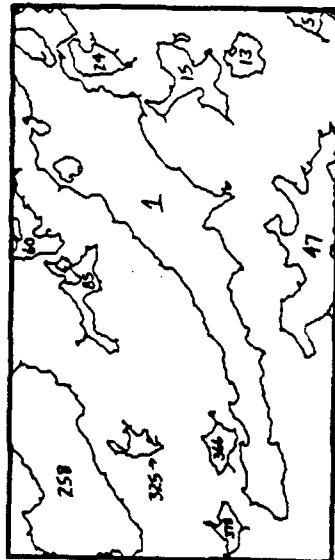


Figure 13. As in Fig. 7 except for Oct. 16, 1983 case.

Figure 12. As in Fig. 5 except for Oct. 16, 1983 case.



a



b

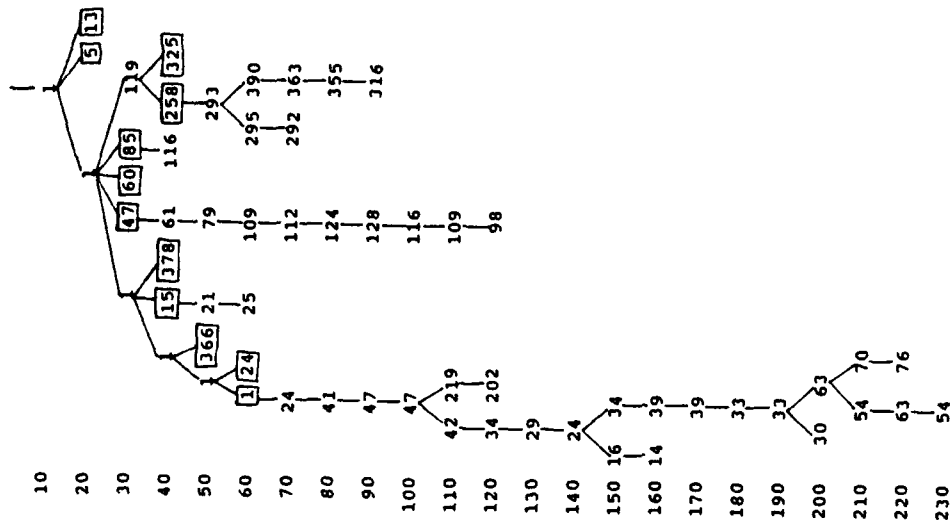
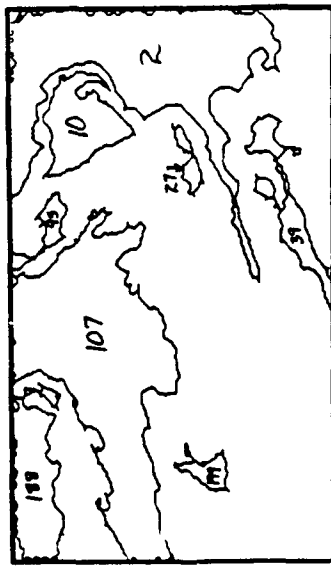


Figure 14. As in Fig. 5 except for Oct. 25, 1983 case.

Figure 15. As in Fig. 7 except for Oct. 25, 1983 case.



a



b

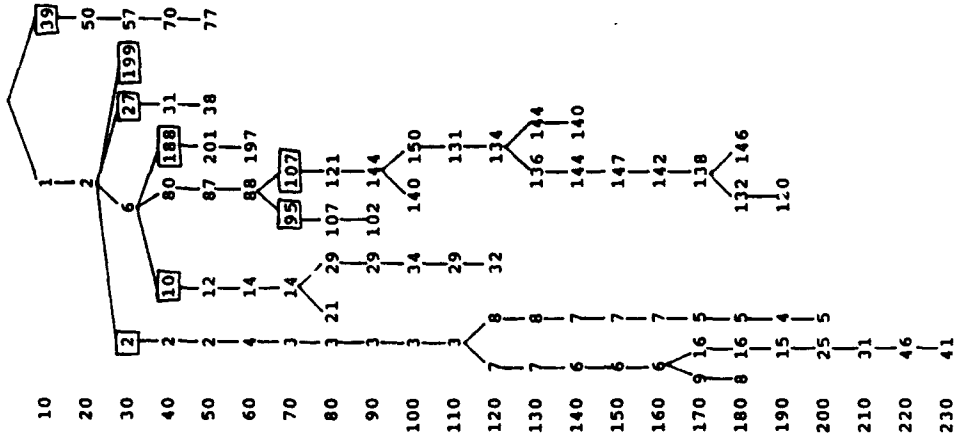
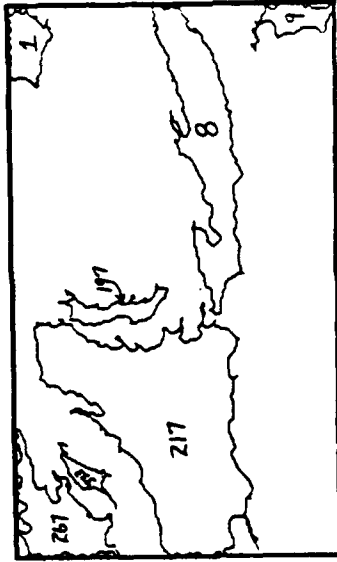


Figure 16. As in Fig. 5 except for Oct. 31, 1983 case.

Figure 17. As in Fig. 7 except for Oct. 31, 1983 case.



a



b

Figure 18. As in Fig. 5 except for Nov. 6, 1983 case.

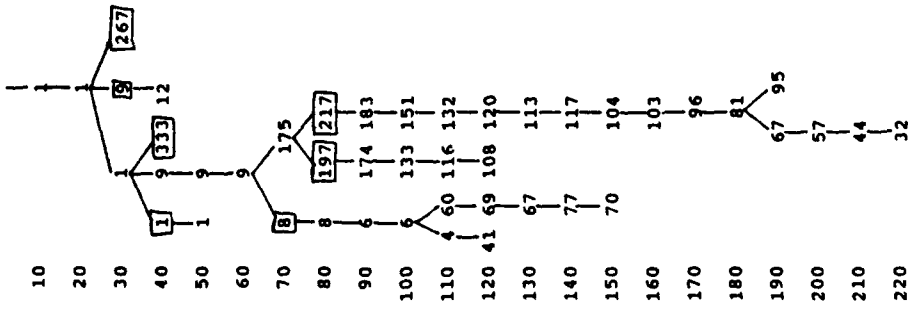


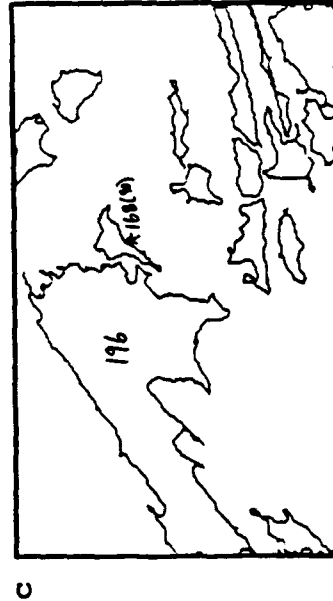
Figure 19. As in Fig. 7 except for Nov. 6, 1983 case.



a



b



c

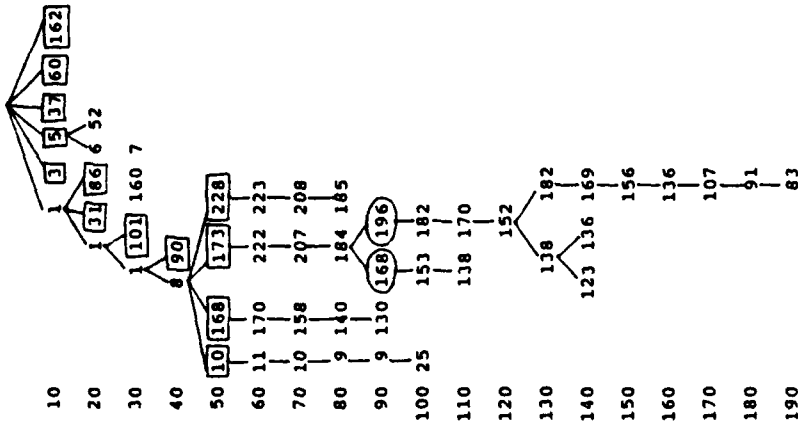


Figure 24. As in Fig. 5 except for Nov. 24, 1983 case.

Figure 25. As in Fig. 7 except for Nov. 24, 1983 case.

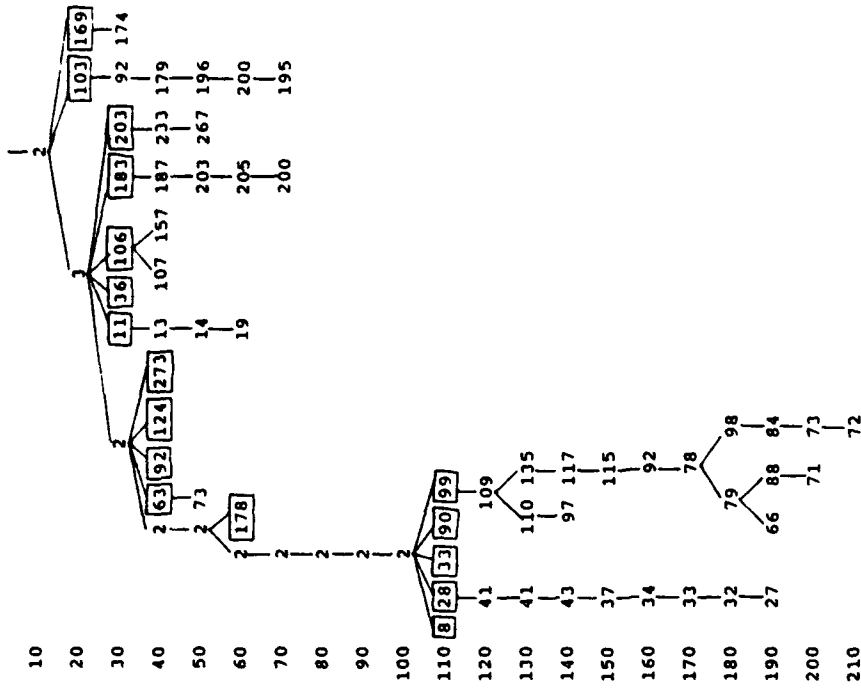
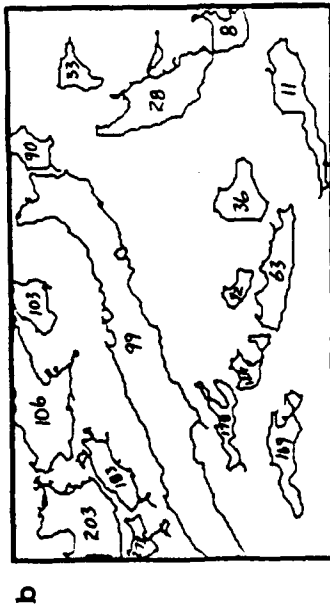
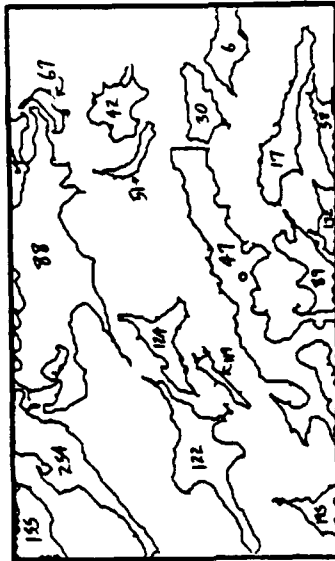


Figure 26. As in Fig. 5 except for Nov. 30, 1983 case.

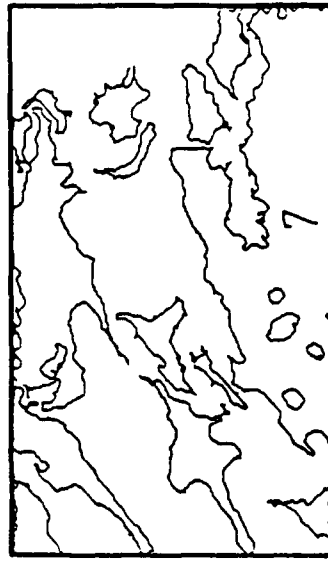
Figure 27. As in Fig. 7 except for Nov. 30, 1983 case.



a



b



c

Figure 30. As in Fig. 5 except for Oct. 13, 1983 case.

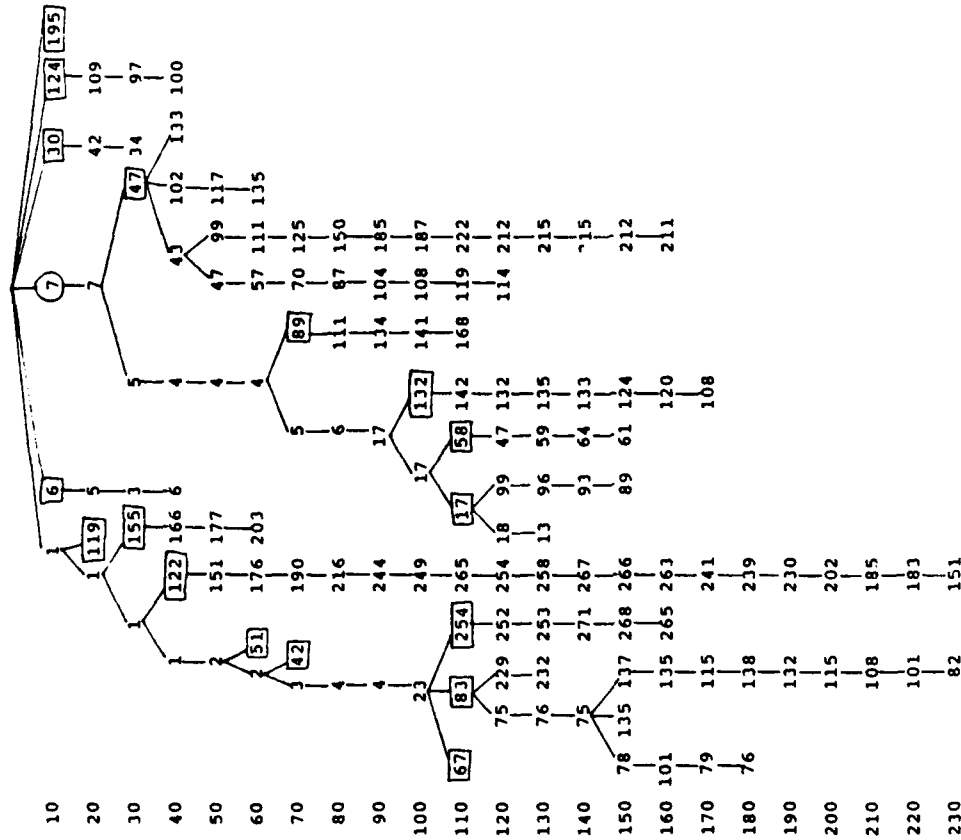


Figure 31. As in Fig. 7 except for Oct. 13, 1983 case.

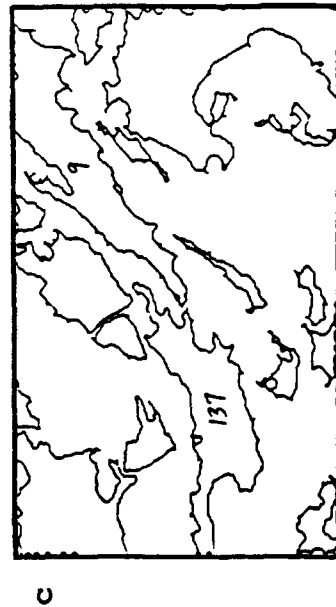
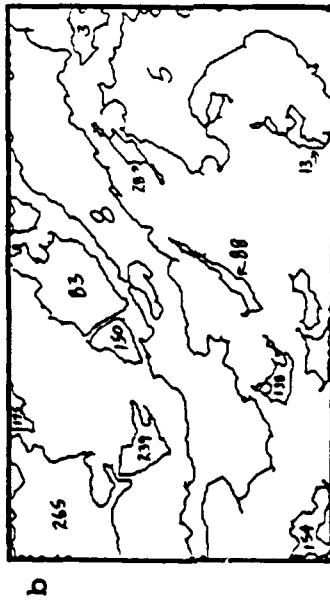


Figure 34. As in Fig. 5 except for Oct. 28, 1983 case.

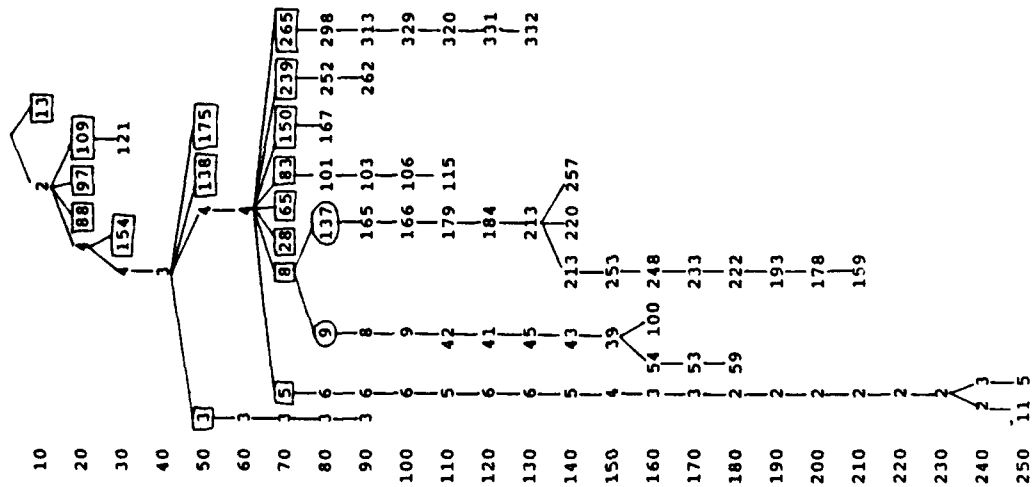
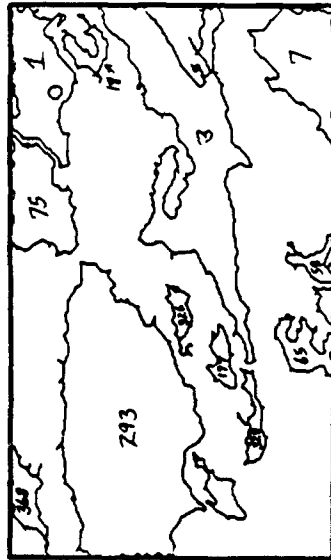


Figure 35. As in Fig. 7 except for Oct. 28, 1983 case.



a



b

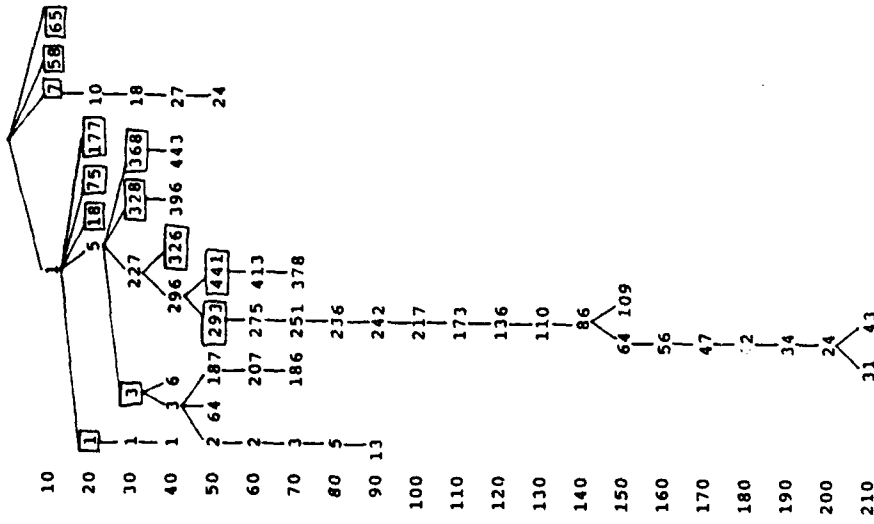


Figure 36. As in Fig. 5 except for Nov. 3, 1983 case.

Figure 37. As in Fig. 7 except for Nov. 3, 1983 case.

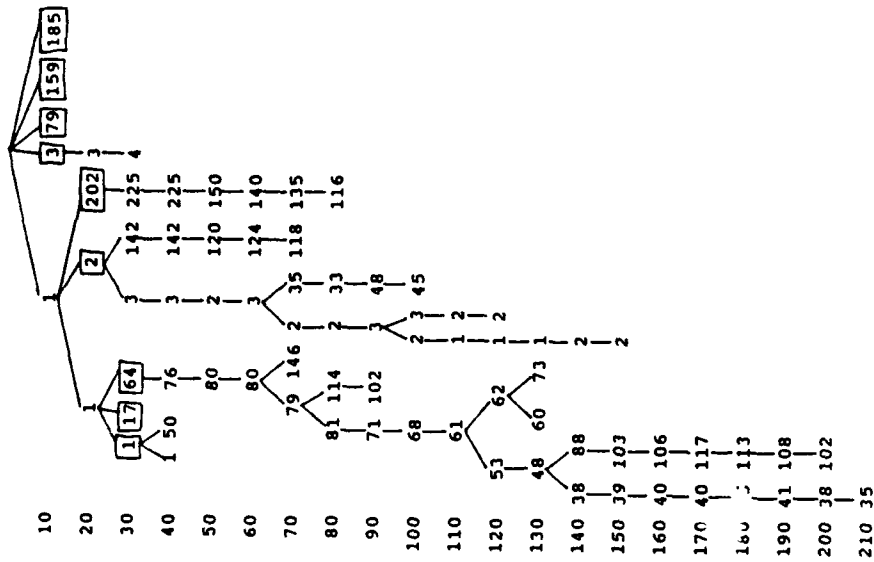
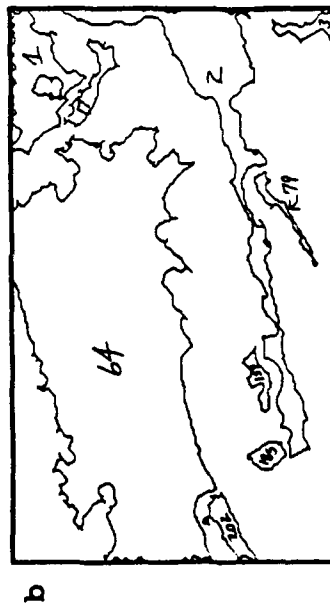
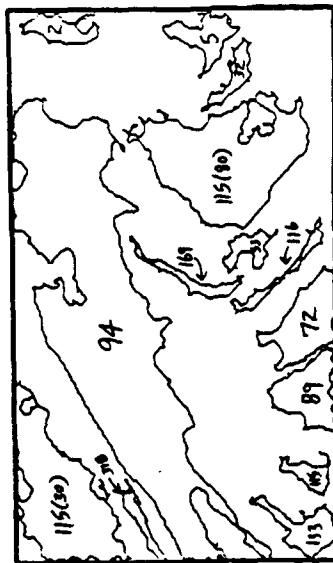


Figure 40. As in Fig. 5 except for Nov. 15, 1983 case.

Figure 41. As in Fig. 7 except for Nov. 15, 1983 case.



a



b

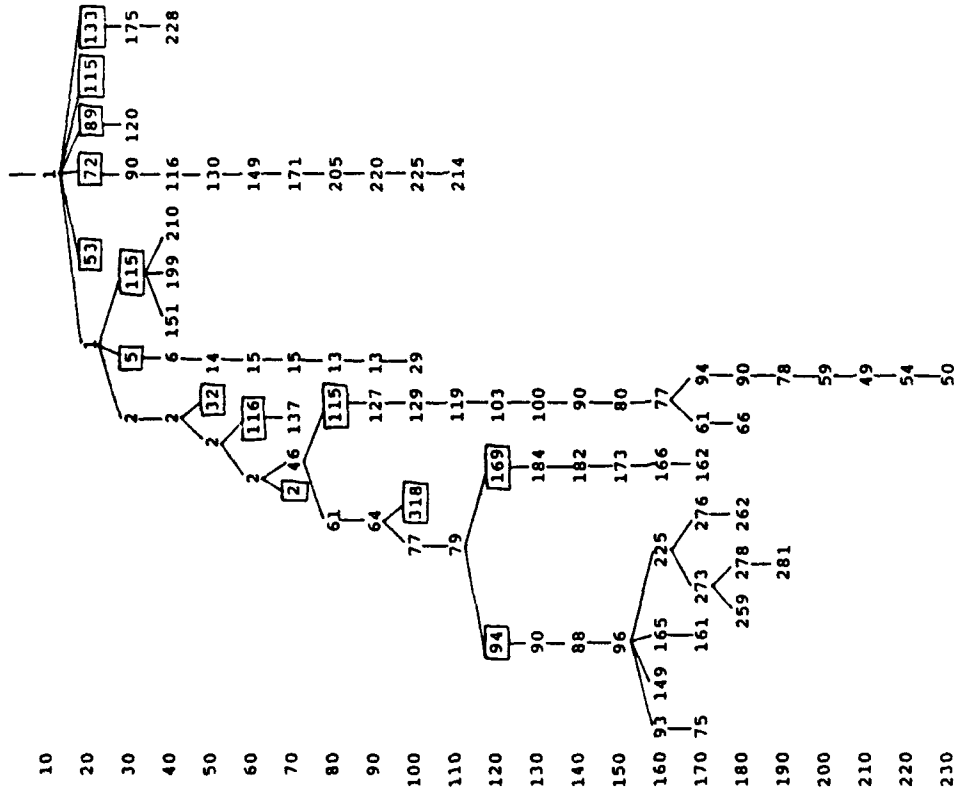


Figure 43. As in Fig. 7 except for Nov. 21, 1983 case.

Figure 42. As in Fig. 5 except for Nov. 21, 1983 case.

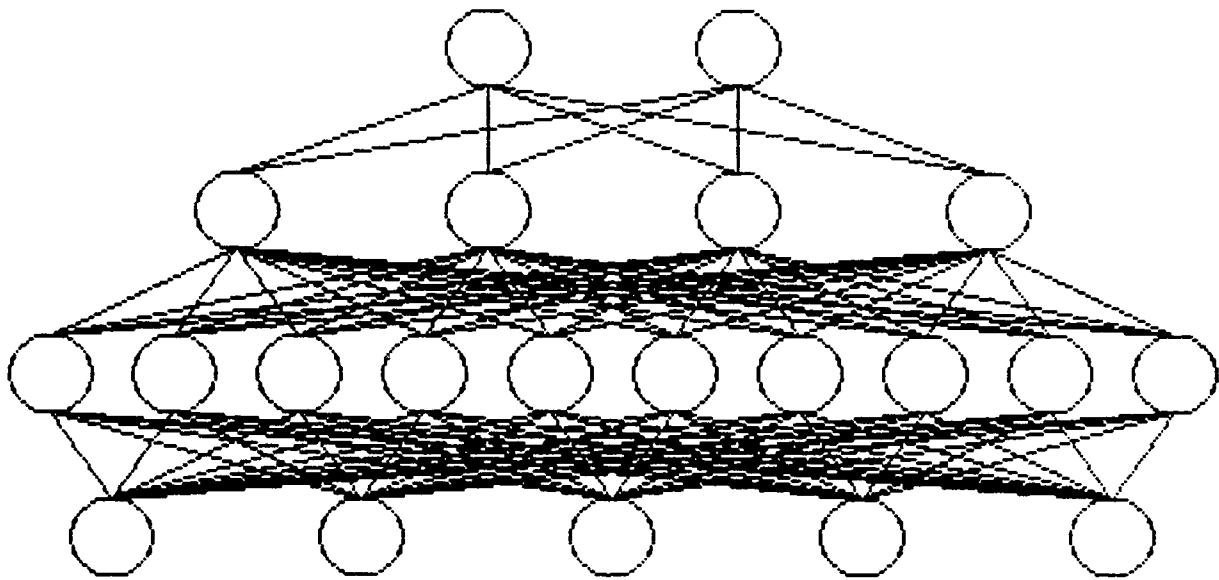


Figure 46. Configuration of feed-forward, back-propagation neural network to select pruning points in hierarchical threshold trees. Circles represent artificial neurons with inputs represented by lines converging from below. Five input nodes (bottom row) feed to 10 nodes in the first hidden layer, four nodes in the second hidden layer, and two output nodes.

DISTRIBUTION LIST

NOARL
ATTN: CODE 104
JCSSC, MS 39529-5004

CHIEF OF NAVAL OPERATIONS
ATTN: OP-096, OP-0961B
U.S. NAVAL OBSERVATORY
WASHINGTON, DC 20392-1800

NOARL
ATTN: CODE 125L (10)
JCSSC, MS 39529-5004

NOARL
ATTN: CODE 125P
JCSSC, MS 39529-5004

NOARL
ATTN: CODE 300
JCSSC, MS 39529-5004

OFFICE OF NAVAL RESEARCH
ATTN: CODE 10
800 N. QUINCY ST.
ARLINGTON, VA 22217-5000

DIRECTOR
WOODS HOLE OCEANOGRAPHIC INST.
P.O. BOX 32
WOODS HOLE, MA 02543

UNIVERSITY OF CALIFORNIA
SCRIPPS INST. OF OCEANOGRAPHY
BOX 6049
SAN DIEGO, CA 92106

OFFICE OF NAVAL TECHNOLOGY
ATTN: DR. P. SELWYN, CODE 20
800 N. QUINCY ST.
ARLINGTON, VA 22217-5000

OFFICE OF NAVAL TECHNOLOGY
DR. M. BRISCOE, CODE 22B
800 N. QUINCY ST.
ARLINGTON, VA 22217-5000

OFFICE OF NAVAL RESEARCH
ATTN: CODE 12
800 N. QUINCY ST.
ARLINGTON, VA 22217-5000

OFFICE OF NAVAL RESEARCH
DR. E. SILVA, CODE 10D/10P
800 N. QUINCY ST.
ARLINGTON, VA 22217-5000

OFFICER IN CHARGE
NAVOCEANCOMDET
AFGWC
OFFUTT AFB, NE 68113

NOARL
ATTN: A. PRESSMAN, CODE 321
JCSSC, MS 39529-5004

COMNAVOCEANCOM
ATTN: CODE N5
JCSSC, MS 39529-5000

U.S. NAVAL ACADEMY
ATTN: OCEANOGRAPHY DEPT.
ANNAPOLIS, MD 21402

NAVAL POSTGRADUATE SCHOOL
ATTN: CODE MR
MONTEREY, CA 93943-5000

NAVAL POSTGRADUATE SCHOOL
ATTN: CODE OC
MONTEREY, CA 93943-5000

NAVAL POSTGRADUATE SCHOOL
ATTN: 0142 (LIBRARY)
MONTEREY, CA 93943-5002

NAVAIRSYSCOM
ATTN: CODE 526W
WASHINGTON, DC 20361-0001

SPAWARSYSCOM
ATTN: CODE 312
NAT. CTR. #1
WASHINGTON, DC 20363-5100

SPAWARSYSCOM
ATTN: CODE PMW-141
NAT. CTR. #1
WASHINGTON, DC 20363-5100

PACMISTESTCEN
ATTN: GEOPHYSICS OFFICER
PT. MUGU, CA 93042

AFGWC/DAPL
ATTN: TECH. LIBRARY
OFFUTT AFB, NE 68113

AFGL/LY
ATTN: MET. OFFICER
HANSCOM AFB, MA 01731

COMMANDING OFFICER
U.S. ARMY RESEARCH OFFICE
ATTN: GEOPHYSICS DIV.
P.O. BOX 12211
RESEARCH TRIANGLE PARK, NC
27709

COMMANDER/DIRECTOR
ASL, WHITE SANDS
ATTN: SLCAS-AE
WSMR, NM 88002-5501

NOAA-NESDIS LIAISON
ATTN: CODE SC2
NASA-JOHNSON SPACE CENTER
HOUSTON, TX 77058

DIRECTOR
NATIONAL EARTH SAT. SERV/SEL
FB-4, S321B
SUITLAND, MD 20233

OCEANOGRAPHIC SERVICES DIV.
NOAA
6010 EXECUTIVE BLVD.
ROCKVILLE, MD 20852

NATIONAL WEATHER SERVICE
WORLD WEATHER BLDG., RM 307
5200 AUTH ROAD
CAMP SPRINGS, MD 20023

CHIEF
MESOSCALE APPLICATIONS BRANCH
NATIONAL EARTH SAT. SERV.
1225 W. DAYTON
MADISON, WI 53562

DIRECTOR
TECHNIQUES DEVELOPMENT LAB
GRAMAX BLDG.
8060 13TH ST.
SILVER SPRING, MD 20910

DIRECTOR
NATIONAL WEATHER SERVICE
GRAMAX BLDG.
8060 13TH ST.
SILVER SPRING, MD 20910

NCAR
ATTN: LIBRARY ACQUISITIONS
P.O. BOX 3000
BOULDER, CO 80307

HEAD, ATMOS. SCIENCES DIV.
NATIONAL SCIENCE FOUNDATION
1800 G STREET, NW
WASHINGTON, DC 20550

EXECUTIVE SECRETARY, CAO
SUBCOMMITTEE ON ATMOS. SCI.
NATIONAL SCIENCE FOUNDATION
RM. 510, 1800 G. STREET, NW
WASHINGTON, DC 20550

DR. MARVIN DICKERSON
L-262, LLNL
P.O. BOX 808
LIVERMORE, CA 94550

COLORADO STATE UNIVERSITY
ATMOSPHERIC SCIENCES DEPT.
ATTN: DR. WILLIAM GRAY
FORT COLLINS, CO 80523

CHAIRMAN
INSTITUTE OF ATMOS. PHYSICS
UNIV. OF ARIZONA
TUSCON, AZ 85721

SCRIPPS INSTITUTION OF
OCEANOGRAPHY, LIBRARY
DOCUMENTS/REPORTS SECTION
LA JOLLA, CA 92037

ATMOSPHERIC SCIENCES DEPT.
UCLA
405 HILGARD AVE.
LOS ANGELES, CA 90024

WOODS HOLE OCEANO. INST.
DOCUMENT LIBRARY LO-206
WOODS HOLE, MA 02543

CHAIRMAN, METEOROLOGY DEPT.
UNIVERSITY OF OKLAHOMA
NORMAN, OK 73069

CHAIRMAN, METEOROLOGY DEPT.
CALIFORNIA STATE UNIVERSITY
SAN JOSE, CA 95192

COLORADO STATE UNIVERSITY
ATTN: ATMOSPHERIC SCI. DEPT.
FT. COLLINS, CO 80523

NATIONAL CENTER FOR ATMOS.
RSCH., LIBRARY ACQUISITIONS
P.O. BOX 3000
BOULDER, CO 80302

UNIVERSITY OF WASHINGTON
ATMOSPHERIC SCIENCES DEPT.
SEATTLE, WA 98195

CHAIRMAN, METEOROLOGY DEPT.
PENNSYLVANIA STATE UNIV.
503 DEIKE BLDG.
UNIVERSITY PARK, PA 16802

FLORIDA STATE UNIVERSITY
ATTN: METEOROLOGY DEPT.
TALLAHASSEE, FL 32306

UNIVERSITY OF HAWAII
ATTN: METEOROLOGY DEPT.
2525 CORREA ROAD
HONOLULU, HI 96822

ATMOSPHERIC SCIENCES DEPT.
OREGON STATE UNIVERSITY
CORVALLIS, OR 97331

UNIVERSITY OF MARYLAND
METEOROLOGY DEPT.
COLLEGE PARK, MD 20742

CHAIRMAN
METEOROLOGY DEPT.
MASSACHUSETTS INSTITUTE OF
TECHNOLOGY
CAMBRIDGE, MA 02139

CHAIRMAN, METEOROLOGY DEPT.
UNIVERSITY OF UTAH
SAL LAKE CITY, UT 84112

TEXAS A&M UNIVERSITY
METEOROLOGY DEPT.
COLLEGE STATION, TX 77843

ATMOSPHERIC SCIENCES CENTER
DESERT RESEARCH INSTITUTE
P.O. BOX 60220
RENO, NV 89506

ATMOSPHERIC SCI. RSCH. CENTER
NEW YORK STATE UNIV.
1400 WASHINGTON AVE.
ALBANY, NY 12222

THE EXECUTIVE DIRECTOR
AMERICAN METEORO. SOCIETY
45 BEACON ST.
BOSTON, MA 02108

DIRECTOR
WORLD METEOROLOGICAL
ORGANIZATION
CASE POSTALE #5, CH-1211
GENEVA, SWITZERLAND

BUREAU OF METEOROLOGY
ATTN: SROD, NMC
BOX 1289K, GPO MELBOURNE
VICTORIA 3001, AUSTRALIA

LIBRARY, AUSTRALIAN NUMERICAL
METEOROLOGY RESEARCH CENTER
P.O. BOX 5089A
MELBOURNE, VICTORIA, 3001
AUSTRALIA

CHAIRMAN, METEOROLOGY DEPT.
MCGILL UNIVERSITY
805 SHERBROOKE ST., W.
MONTREAL, QUEBEC
CANADA H3A 2K6

DEPARTMENT OF METEOROLOGY
UNIVERSITY OF READING
2 EARLYGATE, WHITEKNIGHTS
READING RG6 2AU
ENGLAND

EUROPEAN SPACE OPERATIONS
ATTN: DR. J. MORGAN, METEO.
SAT. DATA, MANAGEMENT DEPT.
R. BOSCH STR 5 D61 DARMSTADT
FEDERAL REPUBLIC OF GERMANY

INSTITUT FUR METEOROLOGIE
J. GUTENBERG UNIVERSITAT
ATTN: DR. R. JAENICKE
D-65 MAINZ
FEDERAL REPUBLIC OF GERMANY

REPORT DOCUMENTATION PAGE

Form Approved
OMB No. 0704-0188

Public reporting burden for this collection of information is estimated to average 1 hour per response, including the time for reviewing instructions, searching existing data sources, gathering and maintaining the data needed, and completing and reviewing the collection of information. Send comments regarding this burden estimate or any other aspect of this collection of information, including suggestions for reducing this burden, to Washington Headquarters Services, Directorate for Information Operations and Reports, 1215 Jefferson Davis Highway, Suite 1204, Arlington, VA 22202-4302, and to the Office of Management and Budget, Paperwork Reduction Project (0704-0188), Washington, DC 20503.

1. Agency Use Only (<i>Leave blank</i>).	2. Report Date. November 1991	3. Report Type and Dates Covered. Final	
4. Title and Subtitle. Segmentation of Satellite Imagery Using Hierarchical Thresholding and Neural Networks		5. Funding Numbers. Program Element No. 62435N Project No. RM35G82 Task No. 4 Accession No. DN651750	
6. Author(s). James E. Peak		7. Performing Organization Name(s) and Address(es). Computer Sciences Corporation, Monterey, CA 93943-5006 Naval Oceanographic and Atmospheric Research Laboratory Atmospheric Directorate (Attn: Dr. P.M. Tag) Monterey, CA 93943-5006	
8. Performing Organization Report Number. NOARL Technical Note 185		9. Sponsoring/Monitoring Agency Name(s) and Address(es). Office of Naval Research (ONT, Code 22) 800 N. Quincy St. Arlington, VA 22217-5000	
10. Sponsoring/Monitoring Agency Report Number. NOARL Technical Note 185		11. Supplementary Notes.	
12a. Distribution/Availability Statement. Approved for public release; distribution is unlimited.		12b. Distribution Code.	
13. Abstract (<i>Maximum 200 words</i>). A significant task in the automated interpretation of cloud features on satellite imagery is the segmentation of the image into separate cloud features to be identified. A new technique, Hierarchical Threshold Segmentation (HTS) is presented. In HTS, region boundaries are defined over a range of grayshade thresholds. The hierarchy of the spatial relationships between colocated regions from different thresholds is represented in tree form. This tree is pruned, using a neural network, such that the regions of appropriate sizes and shapes are isolated. These various regions from the pruned trees are then collected to form the final segmentation of the entire image.			
14. Subject Terms. Neural network Cloud classification Image segmentation		15. Number of Pages. 61	
16. Price Code.		17. Security Classification of Report. UNCLASSIFIED	
18. Security Classification of This Page. UNCLASSIFIED		19. Security Classification of Abstract. UNCLASSIFIED	
20. Limitation of Abstract. Same as report			